Oxidative Addition to Diplatinum(II) Complexes: Stereoselectivity and Cooperative Effects

Cliff R. Baar, Lee P. Carbray, Michael C. Jennings, and Richard J. Puddephatt*

Department of Chemistry, The University of Western Ontario, London, Canada N6A 5B7

Received February 7, 2000

The stereochemistry of oxidative addition of MeI and MeO_3SCF_3 to binuclear dimethylplatinum(II) complexes containing bis(bidentate) ligands such as *cis*- and *trans*-1,2-C_6H_{10}-(N═CH-2-$C_5H_4N)_2$, **1** and **2a**, has been studied. Oxidative addition of the Me−X bond (X = I or CF_3SO_3) occurred at both dimethylplatinum centers, often with high stereoselectivity, to give bis(trimethylplatinum(IV)) complexes. Two types of adducts were formed, either neutral complexes containing $\{PtMe_3X\}_2$ groups or ionic complexes containing $[(PtMe_3)_2(\mu\text{-}X)]^+X^-$ groups. When X = iodide, both forms were detected, but when X = triflate, the ionic form with one bridging triflate ligand dominated. The triflate ligand was easily displaced by water to give an aqua complex, and reaction of $NaBH_4$ with *cis*-1,2-$[C_6H_{10}\{N{=}CH\text{-}2\text{-}C_5H_4N(PtMe_3)\}_2(\mu\text{-}O_3SCF_3)][O_3SCF_3]$ gave the platinum(IV) borohydride complex *cis*-1,2-$[C_6H_{10}\{N{=}CH\text{-}2\text{-}C_5H_4N(PtMe_3)\}_2(\mu\text{-}BH_4)][O_3SCF_3]$ as a single diastereomer. Addition of PPh_3 to *trans*-1,2-$[C_6H_{10}\{N{=}CH\text{-}2\text{-}C_5H_4N(PtMe_3)\}_2(\mu\text{-}O_3SCF_3)][O_3SCF_3]$ gave C_2-symmetric *trans*-1,2-$[C_6H_{10}\{N{=}CH\text{-}2\text{-}C_5H_4N(PtMe_3PPh_3)\}_2][O_3SCF_3]_2$, with a change in absolute configuration.

Introduction

The use of chiral transition metal complexes to effect organometallic reactions is of fundamental importance in asymmetric catalysis.[1] Since oxidative addition is a key step in several catalytic processes,[2] a better understanding of asymmetric oxidative addition reactions is desirable.[3] Recently it was shown that oxidative addition of alkyl halides, R−I (R = methyl, ethyl, *n*-propyl, and benzyl), to chiral organoplatinum(II) complexes with metalated diimine ligands, derived from *cis*- or *trans*-1,2-diaminocyclohexane, can occur with high stereoselectivity as determined by differences in steric effects (eq 1).[4]

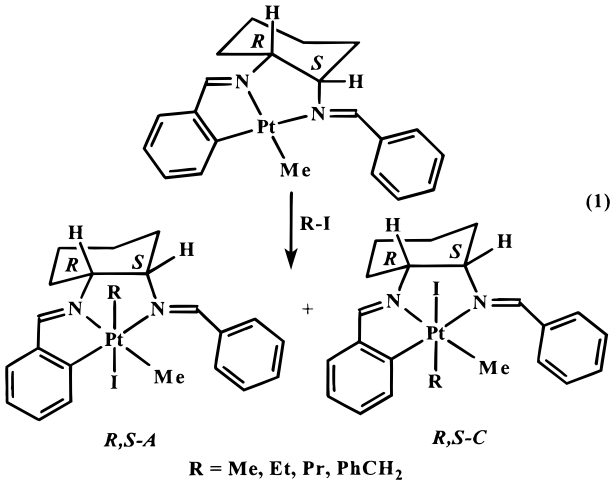

(1)

Modification of the diimine ligands to include a second pair of nitrogen donors allows the bis(bidentate) coordination mode and, thus, formation of organodiplatinum(II) complexes.[5] There is increasing interest in bimetallic systems because cooperative effects, steric or electronic, between the two adjacent metal centers can give rise to reaction pathways or products not possible in the mononuclear analogues.[6] For bridged binuclear complexes, oxidative addition of alkyl halides can yield several types of products, formed by single or double addition.[7] One relevant example that can give double oxidative addition and form products having either *syn* or *anti* stereochemistry is illustrated in eq 2.[8]

For a diplatinum(II) complex with a chiral auxiliary ligand, the faces at each square-planar platinum center

(1) Brunner H. *Angew. Chem., Int. Ed. Engl.* **1999**, *38*, 1194.

(2) Stille, J. K. In *The Chemistry of the Metal−Carbon Bond*; Hartley, F. R., Patai, S., Eds.; Wiley: New York, 1985; Vol. 2, Chapter 9.

(3) (a) Gianini, M.; Forster, A.; Haag, P.; von Zelewsky, A.; Stoeckli-Evans, H. *Inorg. Chem.* **1996**, *35*, 4889. (b) Crespo, M. *Polyhedron* **1996**, *15*, 1981. (c) Baar C. R.; Hill, G. S.; Vittal, J. J.; Puddephatt, R. J. *Organometallics* **1998**, *17*, 32. (d) Crespo, M.; Solans, X.; Font-Bardia, M. *Polyhedron* **1998**, *17*, 3927. (e) Kataoka, Y.; Shibahara, A.; Saito, Y.; Yamagata, T.; Tani, K. *Organometallics* **1998**, *17*, 4338.

(4) Baar, C. R.; Jenkins, H. A.; Vittal, J. J.; Yap, G. P. A.; Puddephatt, R. J. *Organometallics* **1998**, *17*, 2805.

(5) Baar, C. R.; Jennings, M. C.; Puddephatt, R. J.; Muir, K. W. *Organometallics* **1999**, *18*, 4373.

(6) (a) Elduque, A.; Aguilera, F.; Lahoz, F. J.; Lopez, J. A.; Oro, L. A.; Pinillos, M. T. *Inorg. Chim. Acta* **1998**, *274*, 15. (b) Tejel, C.; Bordonaba, M.; Ciriano, M. A.; Edwards, A. J.; Clegg, W.; Lahoz, F. J.; Oro, L. A. *Inorg. Chem.* **1999**, *38*, 1108.

(7) Poilblanc, R. *Inorg. Chim. Acta* **1982**, *62*, 75. (b) Fackler, J. P., Jr.; Murray, H. H.; Basil, J. D. *Organometallics* **1984**, *3*, 821. (c) Schenck, T. G.; Milne, C. R. C.; Sawyer, J. F.; Bosnich, B. *Inorg. Chem.* **1985**, *24*, 2338 (d) Ling, S. S. M.; Jobe, I. R.; Manojlovic-Muir, Lj.; Muir, K. W.; Puddephatt, R. J. *Organometallics* **1985**, *4*, 1198. (e) Schmidbaur, H.; Franke, R. *Inorg. Chim. Acta* **1975**, *13*, 85. (f) Coleman, A. W.; Eadie, D. T.; Stobart, S. R.; Zaworotko, M. J.; Atwood, J. L. *J. Am. Chem. Soc.* **1982**, *104*, 4253. (g) Lewis, N. S.; Mann, K. R.; Gordon, J. G. II; Gray, H. B. *J. Am. Chem. Soc.* **1976**, *98*, 7461. (h) Puddephatt, R. J.; Scott, J. D. *Organometallics* **1985**, *4*, 1221. (i) Meakin, O. P.; Jesson, J. P.; Tolman, C. A. *J. Am. Chem. Soc.* **1972**, *94*, 3240.

(8) Scott, J. D.; Puddephatt, R. J. *Organometallics* **1986**, *5*, 2522.

10.1021/om000108n CCC: $19.00
Publication on Web 05/23/2000

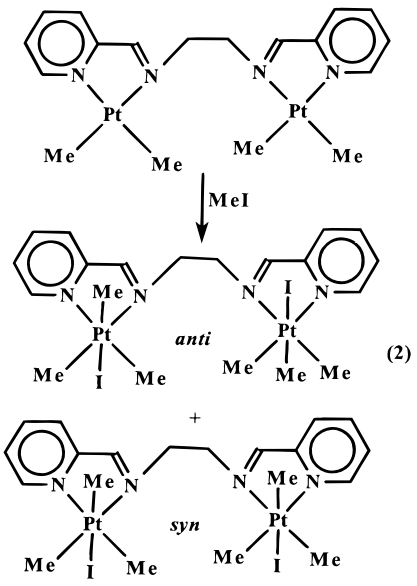

are diastereotopic and give rise to an increased number of potential stereoisomers for oxidative addition reactions. The possible isomers for binuclear platinum complexes supported by ligands based on *cis*- and *trans*-1,2-diaminocyclohexane are outlined schematically in Chart 1. The axial methyl ligands may be coordinated in an up/up or down/down *syn* arrangement or an up/down or down/up *anti* configuration to give four possible permutations, but, for either ligand, internal symmetry reduces the total number of possible isomers to three (Chart 1).[9] Thus, in complexes of the *cis* ligand, *anti* additions are related by a mirror plane and form a racemic mixture (*R,S-A,A/S,R-C,C*) and, for the *trans* ligand, a C_2 rotation axis makes *syn* additions equivalent (Chart 1). For the *cis* ligand, only *anti* addition gives a chiral isomer, but for the *trans* ligand all possible isomers are chiral. However, since the ligand used was either the *cis meso* form or *trans* racemic form, all chiral products were formed as racemic mixtures (for selected products, the enantiomeric forms are shown in parentheses in Chart 1).

This article reports the oxidative addition reactions of methyl iodide and methyl triflate to diplatinum(II) complexes and shows that cooperative effects between neighboring platinum centers together with differential steric effects can lead to very high stereoselectivity. In addition, it is shown that the diastereomerically pure diplatinum(IV) products, which are formed by oxidative addition of methyl triflate, can be used as precursors to new chiral diplatinum(IV) complexes, including the first platinum(IV) borohydride complex.[10,11]

Results

Diplatinum(II) Complexes. The bis(bidentate) ligands *cis*- and *trans*-1,2-C_6H_{10}(N=CH-2-C_5H_4N)$_2$ (C_5H_4N = pyridyl), **1** and **2a**, and their diplatinum(II) complexes, *cis*- and *trans*-1,2-[C_6H_{10}{N=CH-2-C_5H_4N-(PtMe$_2$)}$_2$], **3** and **4**, respectively, have been reported.[5] The new racemic ligands *trans*-1,2-C_6H_{10}(N=CH-2-MeC_5H_3N)$_2$, **2b** (MeC_5H_3N = 6-methylpyridyl), and *trans*-1,2-C_6H_{10}(N=CH-2-C_9H_6N)$_2$, **2c** (C_9H_6N = quinolyl), were prepared similarly by condensation of racemic *trans*-1,2-diaminocyclohexane with 6-methyl-2-pyridinecarboxaldehyde or 2-quinolinecarboxaldehyde, respectively. In both cases the imine bonds have *anti* stereochemistry. Complexes *R,R/S,S-trans*-1,2-[C_6H_{10}-{N=CH-2-MeC_5H_3N(PtMe$_2$)}$_2$], **5**, and *R,R/S,S-trans*-1,2-[C_6H_{10}{N=CH-2-C_9H_6N(PtMe$_2$)}$_2$], **6**, were prepared by reaction of [PtMe$_2$(μ-SMe$_2$)]$_2$ with a stoichiometric amount of ligand **2b** or **2c** in diethyl ether solution. Ligands analogous to **2b** and **2c** were prepared from *cis*-1,2-diaminocyclohexane, but attempts to synthesize diplatinum(II) complexes analogous to **3** from them failed, presumably due to larger steric interactions in the substituted *cis*-ligand complexes.

The ^{1}H NMR spectra of **5** and **6** show that the complexes have C_2 symmetry. For example, complex **5** gives methylplatinum(II) resonances at δ = 1.50 and 1.80, with ^2J(PtH) = 90 and 84 Hz, respectively, and a single imine resonance at δ = 9.56, with ^3J(PtH) = 33 Hz. The C_s-symmetric complex **3** and the chiral C_2-symmetric (but racemic *R,R/S,S*) complexes **4**−**6** are illustrated in Chart 2.

Oxidative Addition of Methyl Iodide. The reaction of *cis*-1,2-[C_6H_{10}{N=CH-2-C_5H_4N(PtMe$_2$)}$_2$], **3**, with excess methyl iodide at room temperature initially gives a mixture of two diplatinum(IV) products, **7a** and **7b**, but after 1 h, only **7b** is present. When the reaction was monitored by ^{1}H NMR spectroscopy at −70 °C, the earliest detectable species was **7a**, and it was formed in essentially quantitative yield. Complex **7a** persisted in solution until the temperature was raised to −20 °C, when isomerization to **7b** began. Continued slow warming to ambient temperature effected complete isomerization to the final product, **7b**.

The ^{1}H NMR spectrum of **7a** showed six equal intensity methylplatinum(IV) resonances and two imine resonances, indicative of a single asymmetric isomer. There were two methylplatinum resonances at higher field, δ = 0.59 and 0.80, both with ^2J(PtH) = 72 Hz, due to methyl ligands *trans* to iodide and four singlets further downfield at δ = 1.41−1.54, all with ^2J(PtH) = 71 Hz, due to methyl ligands *trans* to the imine and pyridyl groups.[3c,4,5] The imine resonances were present at δ = 9.32 and 9.79, with ^3J(PtH) = 28 and 27 Hz, respectively. The loss of C_s symmetry on formation of

(9) For chirality descriptors see: Block, B. P.; Powell, W. H.; Fernelius, W. C. *Inorganic Nomenclature: Principles and Practice*; American Chemical Society: Washington, DC, 1990; Chapter 16. In these complexes, the order of descriptors is such that for a complex with descriptor *R,S-C,A* one nitrogen atom will be bound to both the *R* carbon and *C* platinum center and another to both the *S* carbon and *A* platinum center.

(10) (a) Holah, D. G.; Hughes, A. N.; Maciaszek, S.; Magnuson, V. R. *J. Chem. Soc., Chem. Commun.* **1983**, 1308. (b) Green, B. E.; Kennard, C. H. L.; Smith, G.; James, B. D.; Healy, P. C.; White. A. H. *Inorg. Chim. Acta* **1984**, *81*, 147. (c) Mancini, M.; Bougeard, P.; Burns, R. C.; Mlekuz, M.; Sayer, B. G.; Thompson, J. I. A.; McGlinchey, M. J. *Inorg. Chem.* **1984**, *23*, 1072. (d) Shinomoto, R.; Brennan, J. G.; Edelstein, N. M.; Zalkin, A. *Inorg. Chem.* **1985**, *24*, 2896. (e) Rhodes, L. F.; Venanzi, L. M.; Sorato, C.; Albinati, A. *Inorg. Chem.* **1986**, *25*, 3335. (f) Carreno, R.; Riera, V.; Ruiz, M. A.; Jeannin, Y.; Philoche-Levisalles, M. *J. Chem. Soc., Chem. Commun.* **1990**, 15. (g) Lobkovsky, E. B.; Gun'ko, Y. K.; Bulychev, B. M.; Belsky, V. K.; Soloveichik, G. L.; Antipin, M. Y. *J. Organomet. Chem.* **1991**, *406*, 343. (h) Reger, D. L.; Collins, J. E.; Matthews, M. A.; Rheingold, A. L.; Liable-Sands, L. M.; Guzei, I. A. *Inorg. Chem.* **1997**, *36*, 6266. (i) Kasani, A.; Gambarotta, S.; Bensimon, C. *Can. J. Chem.* **1997**, *75*, 1494. (j) Stewart, P. J.; Blake, A. J.; Mountford, P. *Organometallics* **1998**, *17*, 3271. (k) Cendrowski-Guillaume, S. M.; Nierlich, M.; Lance, M.; Ephritikhine, M. **1998**, *17*, 786. (l) Cotton, F. A.; Murillo, C. A.; Wang, X. *J. Am. Chem. Soc.* **1998**, *120*, 9594.

(11) Marks, T. J.; Kolb, J. R.; *Chem. Rev.* **1977**, *77*, 263.

Chart 1

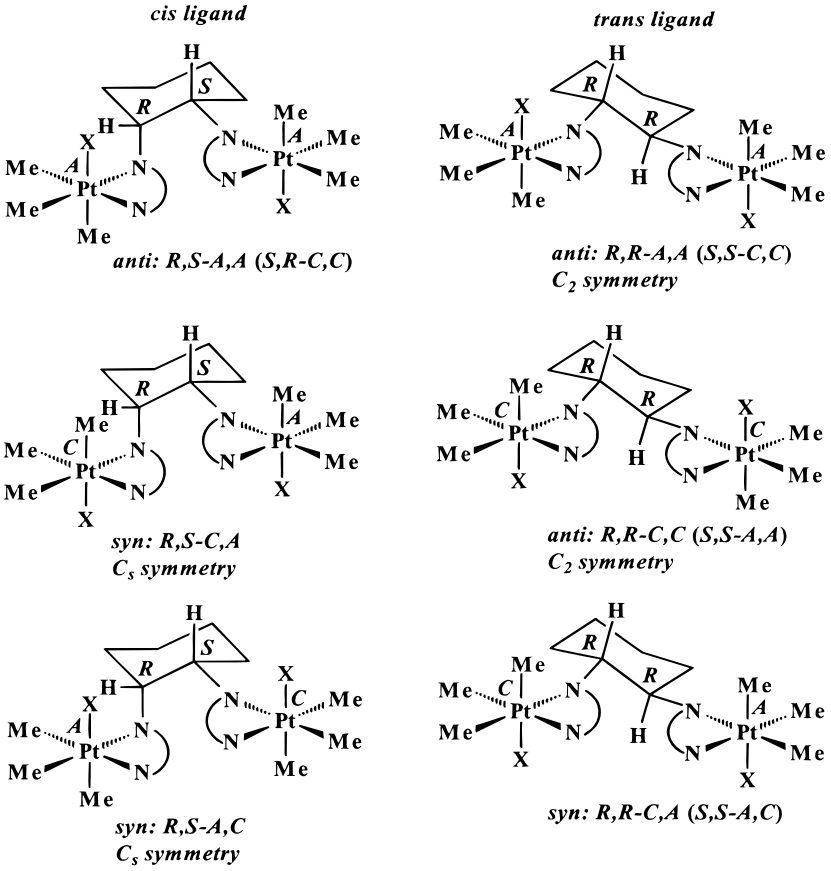

Chart 2

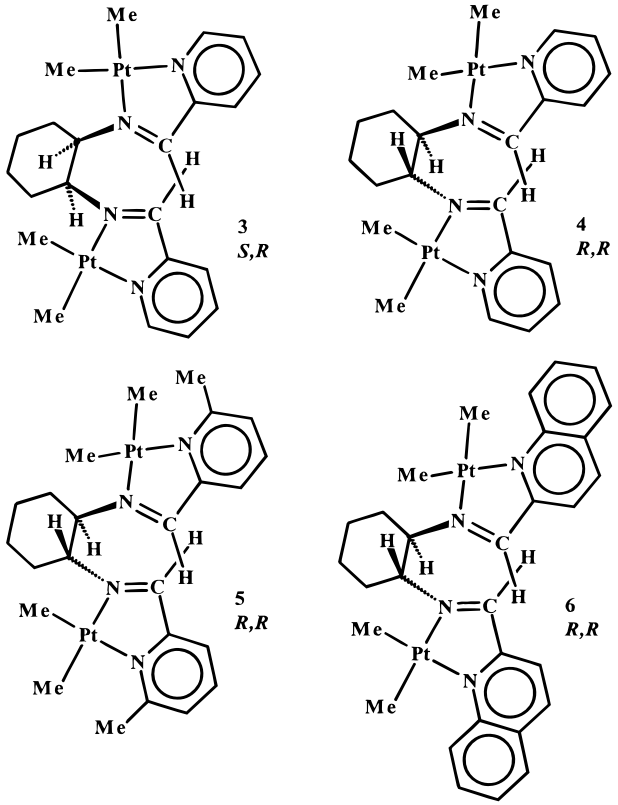

Scheme 1

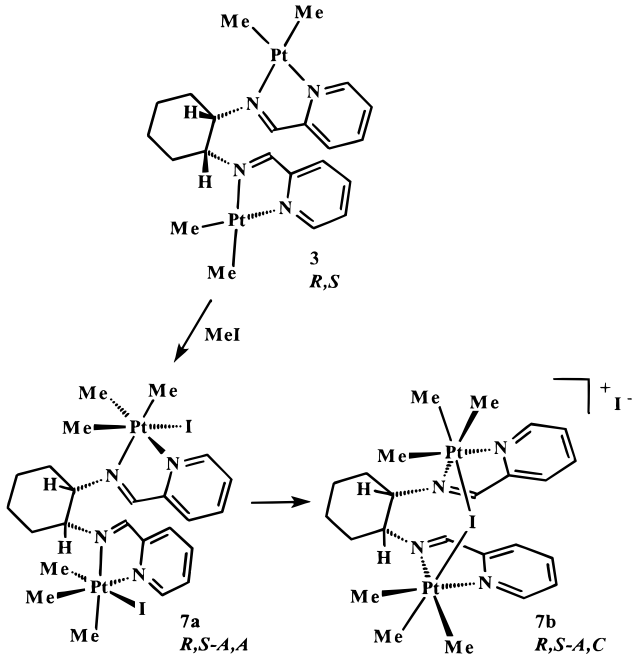

7a is consistent with oxidative addition at each platinum(II) center to give the *anti* stereochemistry shown in Scheme 1.[8] Complex **7a** is chiral but is necessarily formed as a racemic mixture, where the enantiomers have absolute configurations *R,S-A,A* and *S,R-C,C*.[9]

The ^{1}H NMR spectrum of complex **7b** indicated the formation of a single diastereomer with C_s symmetry. The spectrum showed a resonance at $\delta = 0.72$, with ^2J(PtH) = 76 Hz, for the methylplatinum(IV) group *trans* to iodide, and resonances at $\delta = 1.27$ and 1.39 with ^2J(PtH) = 68 and 69 Hz, respectively, for the

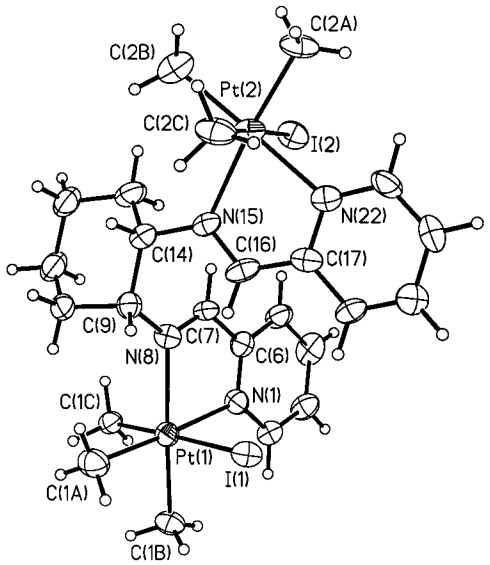

Figure 1. View of the structure of the *R,S-A,A* enantiomer of complex **7a**.

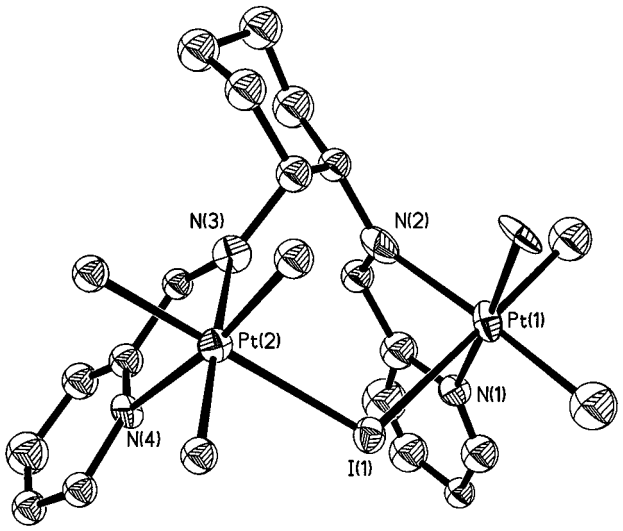

Figure 2. View of the structure of the *R,S-A,C* isomer of the cationic complex **7b**, having approximate C_s symmetry.

Table 1. Selected Bond Distances and Angles for Complex 7a

(a) Bond Distances (Å)

Pt(1)−C(1B)	2.06(1)	Pt(1)−C(1A)	2.07(1)
Pt(1)−C(1C)	2.12(1)	Pt(1)−N(1)	2.160(9)
Pt(1)−N(8)	2.21(1)	Pt(1)−I(1)	2.771(1)
Pt(2)−C(2A)	2.05(1)	Pt(2)−C(2B)	2.06(1)
Pt(2)−C(2C)	2.06(1)	Pt(2)−N(22)	2.17(1)
Pt(2)−N(15)	2.21(1)	Pt(2)−I(2)	2.813(1)
C(7)−N(8)	1.27(2)	N(15)−C(16)	1.27(2)

(b) Bond Angles (deg)

C(1B)−Pt(1)−C(1A)	84.0(5)	C(1B)−Pt(1)−C(1C)	86.1(5)
C(1A)−Pt(1)−C(1C)	90.0(5)	C(1B)−Pt(1)−N(1)	98.5(4)
C(1A)−Pt(1)−N(1)	177.1(5)	C(1C)−Pt(1)−N(1)	88.5(4)
C(1B)−Pt(1)−N(8)	174.9(4)	C(1A)−Pt(1)−N(8)	100.7(5)
C(1C)−Pt(1)−N(8)	91.9(4)	N(1)−Pt(1)−N(8)	76.8(4)
C(1B)−Pt(1)−I(1)	92.7(4)	C(1A)−Pt(1)−I(1)	88.9(4)
C(1C)−Pt(1)−I(1)	178.5(3)	N(1)−Pt(1)−I(1)	92.6(3)
N(8)−Pt(1)−I(1)	89.3(2)	C(2A)−Pt(2)−C(2B)	82.4(6)
C(2A)−Pt(2)−C(2C)	89.1(5)	C(2B)−Pt(2)−C(2C)	84.6(6)
C(2A)−Pt(2)−N(22)	97.3(5)	C(2B)−Pt(2)−N(22)	174.3(5)
C(2C)−Pt(2)−N(22)	89.6(5)	C(2A)−Pt(2)−N(15)	174.1(5)
C(2B)−Pt(2)−N(15)	103.4(5)	C(2C)−Pt(2)−N(15)	91.0(4)
N(22)−Pt(2)−N(15)	76.8(4)	C(2A)−Pt(2)−I(2)	92.4(4)
C(2B)−Pt(2)−I(2)	97.9(4)	C(2C)−Pt(2)−I(2)	177.2(4)
N(22)−Pt(2)−I(2)	87.8(2)	N(15)−Pt(2)−I(2)	87.3(2)

methylplatinum(IV) groups *trans* to imine and pyridyl groups. A single imine resonance is observed at $\delta = 10.14$ with $^3J(\mathrm{PtH}) = 32$ Hz. Restoration of the C_s symmetry in the final product, **7b**, requires rearrangement to the *syn* stereochemistry (Scheme 1, Chart 1). Although *syn* addition requires opposite absolute configurations at each platinum(IV) center, it is not possible to distinguish between the *R,S-A,C* and *R,S-C,A* diastereomeric forms[9] based on the ^{1}H NMR data.

The ^{1}H NMR data are consistent with high stereoselectivity in the oxidative addition of methyl iodide (>99%) to give **7a** as well as stereoselective isomerization (>95%) to the final complex **7b**,[12] but give no information on the absolute stereochemistry of complex **7b**. Furthermore, the spectroscopic data do not distinguish between bonding modes in which an iodide ligand coordinates in a terminal fashion at each platinum atom or to both platinum centers in a bridging Pt(μ-I)Pt arrangement.[13] To make unambiguous stereochemical assignments and to determine the bonding mode of the iodide ligands, complexes **7a** and **7b** were structurally characterized.

A view of the *R,S-A,A* enantiomer of **7a** is provided in Figure 1, and selected bond lengths and angles are given in Table 1. Each platinum(IV) center is octahedrally coordinated by a planar imine/pyridyl chelate, a terminal iodide ligand, and three methyl groups with the expected PtC_3-*facial* geometry in which mutually *trans* carbon donor ligands are avoided.[14] The cyclohexane ring is in the favored chair conformation, minimizing steric interaction between the (N−N)Pt(IV)Me_3I octahedra by forcing them into axial and equatorial positions. The platinum atoms are sufficiently separated, at 7.31 Å, to prevent an iodide ligand from bridging the two metal centers. The structure confirms the *anti* stereochemistry, as predicted on the basis of the ^{1}H NMR data. The absolute configuration of both platinum centers is *anticlockwise* to give overall *R,S-A,A* stereochemistry.[9]

Crystals of complex **7b** were of poor quality, but the data did establish the connectivity, providing a sufficient basis for the discussion of stereochemistry given below. A view of the structure is given in Figure 2 and is very close to that predicted by molecular modeling.[15] The platinum(IV) octahedra are now connected by a bridging iodide ligand, and the complex is cationic; the model predicts that the platinum atoms are now only 4.7 Å apart, while the X-ray structure contains four independent molecules with Pt···Pt distances in the range 4.66−

(12) Wehman-Ooyevaar, I. C. M.; Drenth, W. Grove, D. M.; van Koten, G. *Inorg. Chem.* **1993**, *32*, 3347.

(13) (a) Kuyper, J.; van der Laan, R.; Jeanneaus, F.; Vrieze, K. *Transition Met. Chem.* **1976**, *1*, 199. (b) Scott, J. D.; Puddephatt, R. J. *Organometallics* **1983**, *2*, 1643. (c) Byers, P. K.; Canty, A. J.; Engelhardt, L. M.; White, A. H. *J. Chem. Soc., Dalton Trans.* **1986**, 1731.

(14) (a) Monaghan, P. K.; Puddephatt, R. J. *Organometallics* **1985**, *4*, 1406. (b) Monaghan, P. K.; Puddephatt, R. J. *J. Chem. Soc., Dalton Trans.* **1988**, 595. (c) Anderson, C. M.; Crespo, M.; Jennings, M. C.; Lough, A. J.; Ferguson, G.; Puddephatt, R. J. *Organometallics* **1991**, *10*, 2672. (d) Rendina, L. M.; Puddephatt, R. J. *Chem. Rev.* **1997**, *97*, 1735.

(15) CACHE Scientific Inc., Version 3.7, 1992.

Scheme 2

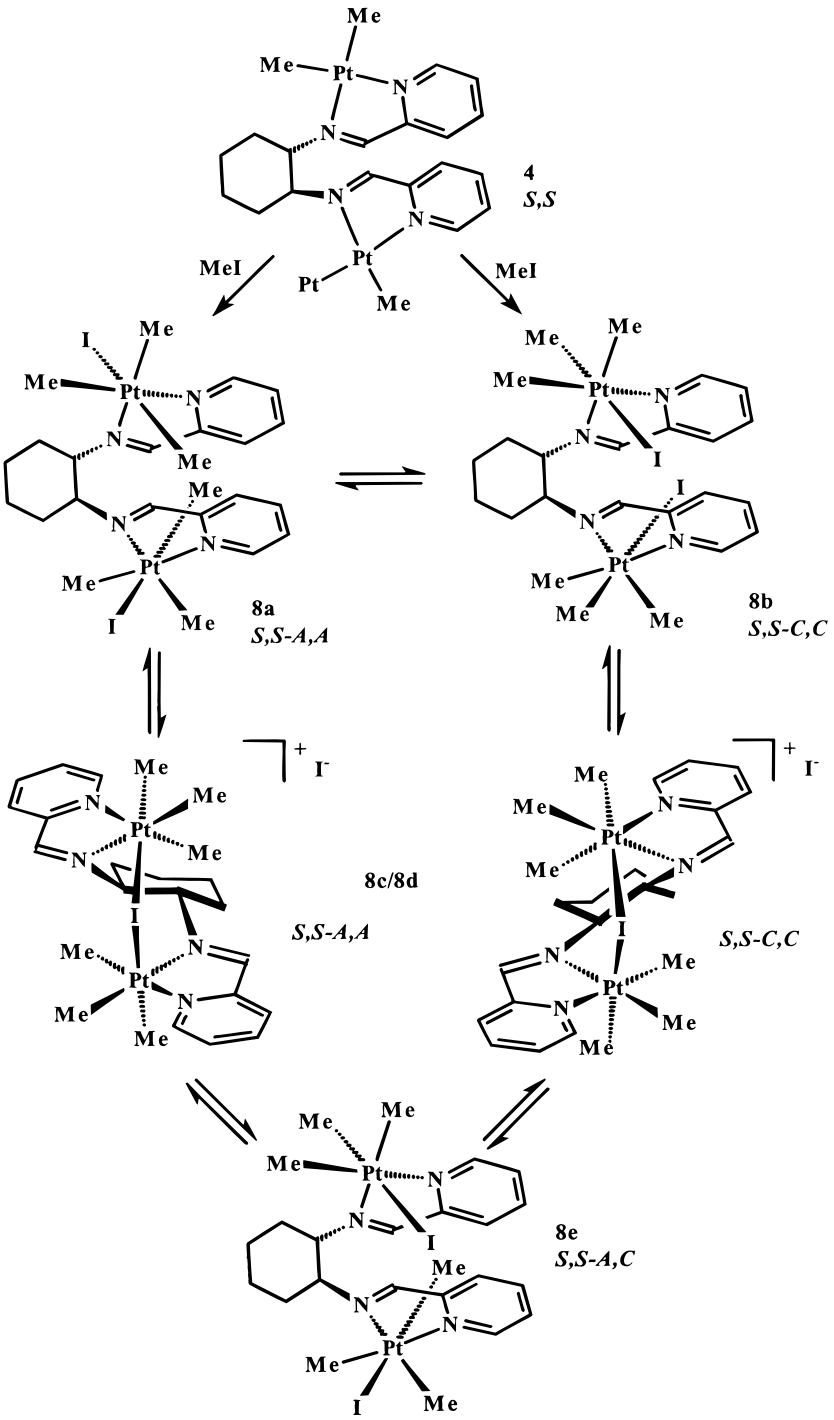

4.75 Å. The complex is close to C_s symmetric, as predicted by ^{1}H NMR spectroscopy. The (N−N)PtMe$_2$ fragments are approximately eclipsed and direct the methyl ligands away from the bulk of the cyclohexane backbone, presumably to minimize steric interactions. The absolute configuration is *R,S-A,C*. In the alternative *syn* configuration, *R,S-C,A*, there would be greater steric congestion since the eclipsed (N−N)PtMe$_2$ fragments would be directed toward the cyclohexane ring, to allow iodide to bridge, and so it is not formed.

Oxidative addition of methyl iodide to **4** was not selective and gave a complex mixture of five products at ambient temperature (Scheme 2). Monitoring the reaction at −70 °C established the order of product formation. The species present in largest amount after short reaction times at low temperature was **8a**. A single set of resonances in the ^{1}H NMR spectrum with three methylplatinum(IV) signals and one imine signal confirmed a C_2-symmetric diplatinum(IV) complex. The initial formation of a C_2-symmetric isomer, **8a**, is consistent with double oxidative addition with *anti* stereochemistry. Also present in smaller amounts were three other C_2-symmetric Pt(IV) products, **8b**−**d** (Scheme 2). Complex **8b** was deduced to be a complex with terminal iodide ligands on each platinum atom, and this was later confirmed by an X-ray structure determination (see below). The first formed diplatinum(IV) species, **8a**, is probably a diastereomer of **8b**. Complexes **8c** and

Scheme 3

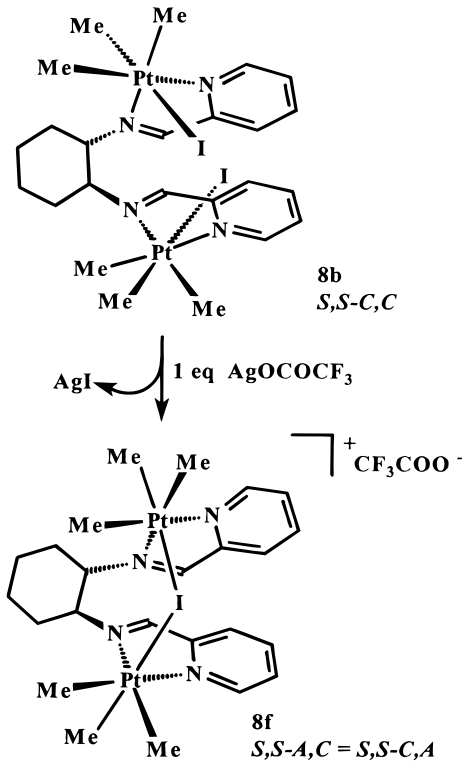

8d are tentatively assigned as a pair of diastereomers having a bridging iodide ligand between the platinum(IV) centers. Finally, trace amounts of a fifth species were observable, and the ^{1}H NMR parameters suggest an asymmetric complex, **8e**, as indicated by the presence of six methylplatinum(IV) resonances and two imine resonances. On warming the solution to room temperature, the resonances due to **8a** decreased rapidly, with only traces remaining after 2 h. The resonances for complexes **8c** and **8d** also decayed but more slowly, requiring a day to decrease to trace amounts. The signals due to **8b** and **8e** increased over this period, and the ratio **8b/8e** was ca. 1:1 after 15 h. However, after several days only **8b** remained in significant amounts. If the reaction was carried out in concentrated solution, complex **8b** slowly precipitated in pure form from the reaction mixture. Pure **8b** was stable for several days when dissolved in CD_2Cl_2, and it is therefore the thermodynamically favored isomer of the oxidative addition reaction.

The addition of an equimolar amount of silver trifluoroacetate to a solution of **8b** caused rapid precipitation of AgI and gave the new complex **8f** (Scheme 3). When the reaction was monitored by ^{1}H NMR, an intermediate can be detected that is asymmetric and appears to contain coordinated trifluoroacetate [^2J(PtH) for MePt = 78 Hz (methyl *trans* to $OCOCF_3$) vs 70 Hz (methyl *trans* to I)]. The intermediate is short-lived and does not build up in significant amounts. The NMR spectra of **8f** are different from any of the complexes in Scheme 2, showing that the cation in **8f** is not formed directly by methyl iodide oxidative addition to **4**.

The structures of **8b** and **8f** were confirmed by X-ray methods. A view of the structure of **8b** is shown in Figure 3, and selected bond distances and angles are given in Table 3. The absolute configuration of complex

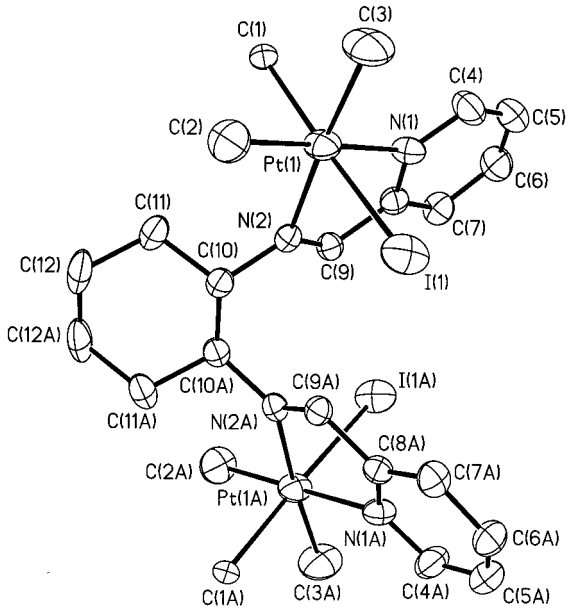

Figure 3. View of the structure of the *S,S-C,C* enantiomer of complex **8b**, having approximate C_2 symmetry.

Table 2. Selected Bond Distances and Angles for Complex 8b[a]

(a) Bond Distances (Å)

Pt(1)−C(2)	2.049(11)	Pt(1)−C(3)	2.079(12)
Pt(1)−N(1)	2.151(8)	Pt(1)−N(2)	2.177(7)
Pt(1)−C(1)	2.216(8)	Pt(1)−I(1)	2.7368(9)
N(2)−C(9)	1.262(11)	N(2)−C(10)	1.474(11)
C(8)−C(9)	1.478(12)		

(b) Bond Angles (deg)

C(2)−Pt(1)−C(3)	84.6(6)	C(2)−Pt(1)−N(1)	177.4(5)
C(3)−Pt(1)−N(1)	97.6(5)	C(2)−Pt(1)−N(2)	101.1(4)
C(3)−Pt(1)−N(2)	174.3(4)	N(1)−Pt(1)−N(2)	76.7(3)
C(2)−Pt(1)−C(1)	89.2(5)	C(3)−Pt(1)−C(1)	85.4(5)
N(1)−Pt(1)−C(1)	89.7(3)	N(2)−Pt(1)−C(1)	94.6(3)
C(2)−Pt(1)−I(1)	90.1(4)	C(3)−Pt(1)−I(1)	90.7(5)
N(1)−Pt(1)−I(1)	91.1(2)	N(2)−Pt(1)−I(1)	89.3(2)
C(1)−Pt(1)−I(1)	176.1(2)		

[a] Symmetry transformations used to generate equivalent atoms: #1 $-x+2, y, -z+3/2$.

8b is *S,S-C,C*. The cyclohexane ring is the chair conformation with (N−N)PtMe$_3$I units occupying equatorial positions. The (N−N)PtMe$_2$ fragments are staggered, and the complex lies on a C_2 axis of symmetry which bisects bonds C10−C10a and C12−C12a. The platinum(IV) octahedra have a *fac*-PtC$_3$ arrangement of methyl ligands, and the axial methyl ligands are *anti* to one another. The Pt−Pt internuclear distance is slightly smaller in **8b** relative to **7a** at 7.10 Å.

The structure of complex **8f** is shown if Figure 4, and selected bond distances and angles are shown in Table 3. The presence of a bridging iodide ligand is confirmed, and the absolute configuration is *R,R-A,C* (note that the enantiomer is *S,S-C,A*). Clearly, formation of **8f** from **8b** requires a change in configuration at one of the platinum centers to allow formation of the bridging iodide. The structural features are similar to those observed for structure **7b**, namely, an eclipsed arrangement for the (N−N)PtMe$_3$ units which makes the complex asymmetric and a much smaller internuclear separation between the platinum atoms of 4.75 Å compared to complexes **7a** and **8b**.

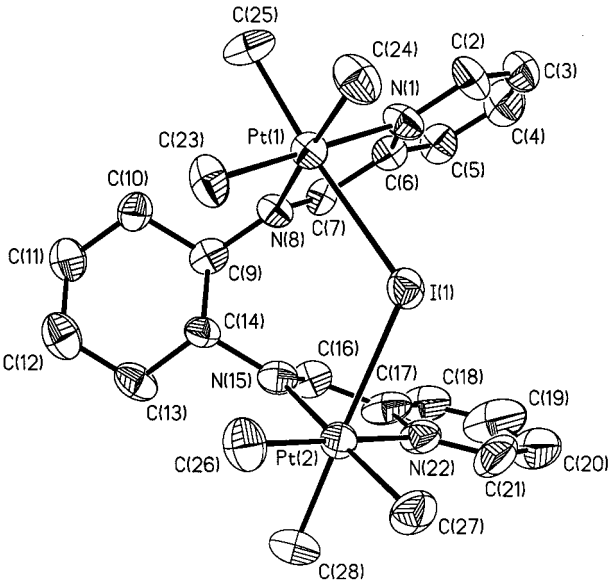

Figure 4. View of the structure of the *R,R-A,C* enantiomer of the cationic complex **8f**.

Table 3. Selected Bond Distances and Angles for Complex 8f

(a) Bond Distances (Å)

Pt(1)−C(24)	2.03(2)	Pt(1)−C(25)	2.05(2)
Pt(1)−C(23)	2.07(1)	Pt(1)−N(1)	2.16(1)
Pt(1)−N(8)	2.237(9)	Pt(1)−I(1)	2.798(1)
Pt(2)−C(28)	2.04(2)	Pt(2)−C(26)	2.04(2)
Pt(2)−C(27)	2.08(2)	Pt(2)−N(15)	2.17(1)
Pt(2)−N(22)	2.17(1)	Pt(2)−I(1)	2.789(1)
C(7)−N(8)	1.26(2)	N(15)−C(16)	1.25(2)

(b) Bond Angles (deg)

C(24)−Pt(1)−C(25)	88.2(8)	C(24)−Pt(1)−C(23)	85.9(7)
C(25)−Pt(1)−C(23)	90.4(8)	C(24)−Pt(1)−N(1)	95.5(6)
C(25)−Pt(1)−N(1)	89.1(7)	C(23)−Pt(1)−N(1)	178.5(6)
C(24)−Pt(1)−N(8)	172.0(6)	C(25)−Pt(1)−N(8)	89.9(6)
C(23)−Pt(1)−N(8)	101.9(5)	N(1)−Pt(1)−N(8)	76.7(4)
C(24)−Pt(1)−I(1)	88.4(6)	C(25)−Pt(1)−I(1)	175.6(6)
C(23)−Pt(1)−I(1)	92.2(6)	N(1)−Pt(1)−I(1)	88.5(4)
N(8)−Pt(1)−I(1)	93.1(3)	C(28)−Pt(2)−C(26)	87.7(8)
C(28)−Pt(2)−C(27)	88.3(8)	C(26)−Pt(2)−C(27)	85.8(8)
C(28)−Pt(2)−N(15)	89.7(7)	C(26)−Pt(2)−N(15)	100.2(7)
C(27)−Pt(2)−N(15)	173.7(6)	C(28)−Pt(2)−N(22)	89.5(7)
C(26)−Pt(2)−N(22)	174.8(7)	C(27)−Pt(2)−N(22)	98.6(7)
N(15)−Pt(2)−N(22)	75.4(5)	C(28)−Pt(2)−I(1)	178.3(6)
C(26)−Pt(2)−I(1)	94.0(6)	C(27)−Pt(2)−I(1)	91.6(6)
N(15)−Pt(2)−I(1)	90.1(3)	N(22)−Pt(2)−I(1)	88.8(4)
Pt(2)−I(1)−Pt(1)	115.55(4)		

Reaction of methyl iodide with the more sterically demanding complexes **5** and **6** was expected to give higher stereoselectivity, but similar complex mixtures were obtained and the products were not characterized. However, due to the facile isolation of one of the major isomers in the reaction of **6** with MeI, an X-ray crystal structure analysis was possible. Although the ^{1}H NMR showed the initial formation of at least two major isomers, an asymmetric species, **9a**, and a C_2-symmetric product, **9b**, rapid precipitation of the products made it difficult to assign product ratios. Nevertheless, because the C_2-symmetric product was most soluble, it was easily separated and crystallized. A view of the structure of **9b** is given in Figure 5. Selected bond distances and angles are provided in Table 4. The absolute configuration is *S,S-C,C*, and the structure is similar to that observed for complex **8b**. The interplatinum distance is also similar at 7.01 Å.

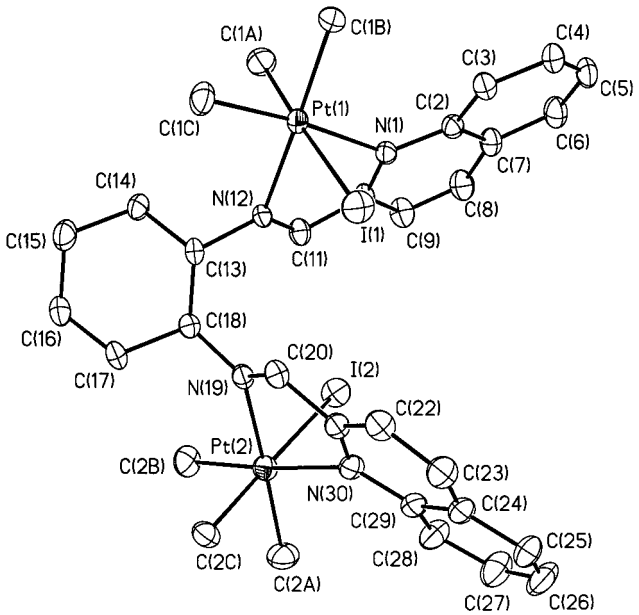

Figure 5. View of the structure of the *S,S-C,C* enantiomer of complex **9b**, having approximate C_2 symmetry.

Table 4. Selected Bond Distances and Angles for Complex 9b

(a) Bond Distances (Å)

Pt(1)−C(1C)	2.057(7)	Pt(1)−C(1B)	2.058(7)
Pt(1)−C(1A)	2.073(8)	Pt(1)−N(12)	2.173(5)
Pt(1)−N(1)	2.218(5)	Pt(1)−I(1)	2.7744(5)
N(19)−Pt(2)	2.185(6)	N(30)−Pt(2)	2.216(5)
Pt(2)−C(2B)	2.043(7)	Pt(2)−C(2A)	2.058(9)
Pt(2)−C(2C)	2.156(8)	Pt(2)−I(2)	2.7545(6)

(b) Bond Angles (deg)

N(12)−Pt(1)−N(1)	75.47(19)	C(10)−N(1)−C(2)	118.7(6)
C(10)−N(1)−Pt(1)	111.3(4)	C(2)−N(1)−Pt(1)	129.6(4)
C(11)−N(12)−C(13)	121.8(5)	C(11)−N(12)−Pt(1)	114.8(4)
C(13)−N(12)−Pt(1)	123.0(4)	C(20)−N(19)−C(18)	122.7(6)
C(20)−N(19)−Pt(2)	113.2(5)	C(18)−N(19)−Pt(2)	123.7(4)
C(21)−N(30)−C(29)	118.0(6)	C(21)−N(30)−Pt(2)	111.6(4)
C(29)−N(30)−Pt(2)	130.1(5)	N(19)−Pt(2)−N(30)	75.3(2)

Oxidative Addition of Methyl Triflate. The reactions of **3**−**6** with methyl triflate at room temperature gave diplatinum(IV) complexes with near perfect stereoselectivity (Schemes 4 and 5). In each case the formation of a single diastereomer of the diplatinum(IV) product was indicated by the ^{1}H NMR data. Reaction of complex **3** with methyl triflate at room temperature in CD_2Cl_2 solution gave product **10**, which was C_s symmetric (Scheme 4). The ^{1}H NMR spectrum showed a methylplatinum resonance at $\delta = 0.74$ with ^2J(PtH) = 84 Hz, consistent with a methylplatinum(IV) groups *trans* to a weakly coordinating triflate ligand,[16] and at $\delta = 1.17$ and 1.18, both with ^2J(PtH) = 66 Hz, due to methylplatinum groups *trans* to the nitrogen donors. The ^{19}F NMR spectrum showed singlets at $\delta = -78.5$ and −78.6, indicating the presence of two chemically distinct triflate ligands which, in a complex of C_s symmetry, must be assigned to coordinated and free triflate ions. The cationic nature of complex **10** was confirmed by an X-ray crystal structure determination (see below).

(16) (a) Hill, G. S.; Vittal, J. J.; Puddephatt, R. J. *Organometallics* **1997**, *16*, 1209. (b) Hill, G. S.; Yap. G. P. A.; Puddephatt, R. J. *Organometallics* **1999**, *18*, 1408.

Scheme 4

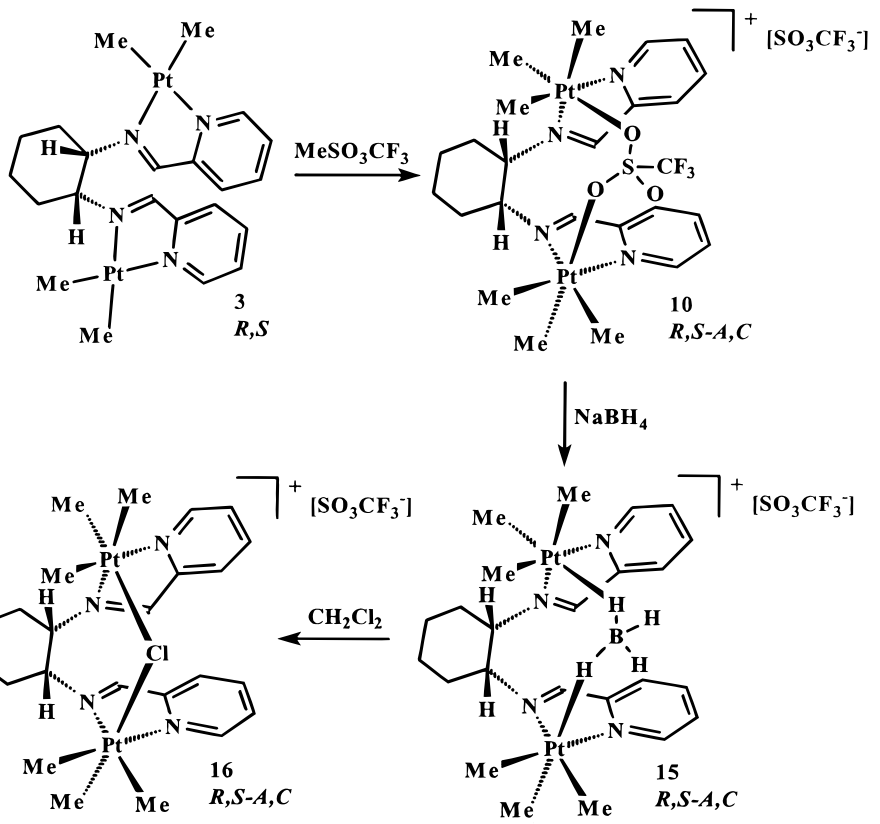

The ^{1}H NMR spectra of complexes **11**−**13**, which are formed by reaction of **4**−**6** respectively with methyl triflate, showed that each was formed as a single asymmetric diastereomer (Scheme 5). In each case, six methylplatinum(IV) resonances and two imine resonances were observed. The two methyl groups *trans* to the triflate ligand had large ^2J(PtH) values of 83−86 Hz, whereas methyl groups *trans* to the nitrogen donors had corresponding smaller ^2J(PtH) values of 66−69 Hz. The ^{19}F NMR spectra showed two singlets for each complex **11**−**13**. A bridging bonding mode for the triflate ligand was established for complex **11** by an X-ray crystal structure determination (see below), and complexes **12** and **13** almost certainly have the same stereochemistry.

A view of the structure of **10** is shown in Figure 6, and selected bond distances and angles are given in Table 5. There are two independent but similar molecules in the cell and only one is illustrated. The structure confirms that a single bridging triflate ligand is present, coordinated to each platinum(IV) atom through two of the oxygen atoms. The absolute configuration is shown to be *R,S-A,C*, analogous to that observed for complex **7b**. All other structural features are very similar to the structure of complex **7b** with the exception of the Pt···Pt internuclear separation, which is significantly larger in the structure for **10** at 5.54 and 5.44 Å in the two independent molecules. Thus, the internuclear cavity expands somewhat to accommodate the larger triflate ligand in complex **10**, showing that the diplatinum unit can serve as host to ligands of different sizes.

If the reaction of **3** with methyl triflate is monitored at −70 °C by ^{1}H NMR spectroscopy, at least one intermediate can be detected, but it quickly isomerizes to complex **10** even at low temperature. A similar sequence of events was observed on route to complex **11** at low temperature, again suggesting that **11** is the product of thermodynamic control. Equilibrium is easily reached by reversible dissociation of the weakly bonded triflate.

The structure of complex **11** is given in Figure 7 with selected bond distances and angles in Table 6. The complex is asymmetric, with a bridging triflate ligand, and has absolute configuration *R,R-A,C*. The Pt−Pt separation is 5.48 Å, similar to complex **10**, but significantly larger than in complex **8f**, which has the same stereochemistry. Once again, the increased internuclear distance is required to accommodate the larger triflate ligand.

Recrystallization of the triflate complex **11** from moist solvent gave the cationic diaqua diplatinum(IV) complex **14** by easy displacement of the bridging triflate ligand by two water molecules. The X-ray crystal structure of **14** was obtained and is shown in Figure 8a. Selected bond distances and angles are given in Table 7. The structure is disordered, since complexes with opposite conformations of the cyclohexane ring are randomly positioned, as shown in Figure 8b. Hence, both diastereomers *R,R-C,C* and *S,S-C,C* are formed when the triflate ligand is replaced by water and both are present in the unit cell. The structural features are similar to those observed for complexes **8b** and **9b** but with a smaller platinum atom separation of 6.32 Å. One aqua ligand, O(1), forms hydrogen bonds to both triflate counterions, O(41) and O(32). The second aqua ligand, O(2), forms a hydrogen bond with a third water molecule, O(50), that is not coordinated.

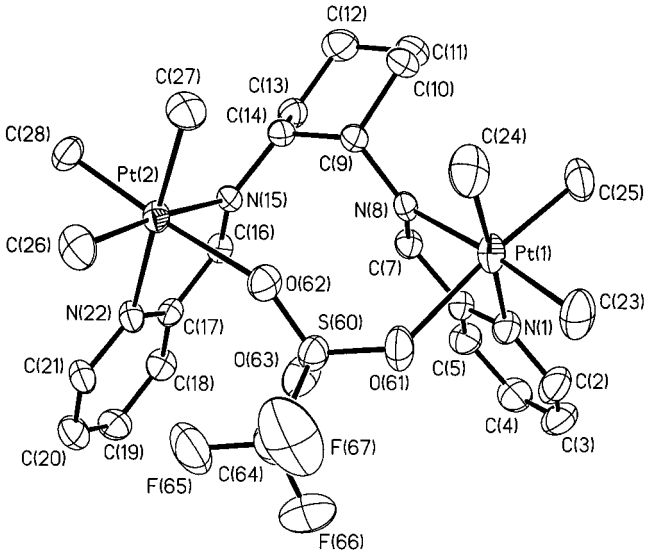

Figure 6. View of the structure of the *R,S-A,C* isomer of the cationic complex **10**, having approximate C_s symmetry.

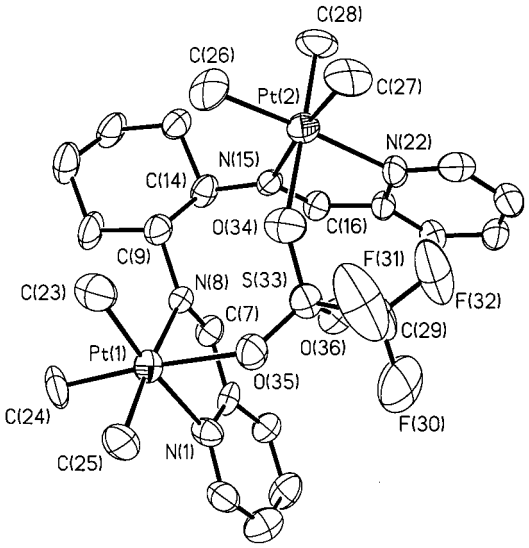

Figure 7. View of the structure of the *R,R-A,C* enantiomer of the cationic complex **11**.

Table 5. Selected Bond Distances and Angles for Complex 10

(a) Bond Distances (Å)

Pt(1)−C(24)	2.025(9)	Pt(1)−C(25)	2.027(8)
Pt(1)−C(23)	2.033(9)	Pt(1)−N(1)	2.147(6)
Pt(1)−N(8)	2.204(5)	Pt(1)−O(61)	2.266(5)
C(7)−N(8)	1.274(8)	N(15)−C(16)	1.266(8)
N(22)−Pt(2)	2.149(5)	Pt(2)−C(28)	2.001(8)
Pt(2)−C(27)	2.041(7)	Pt(2)−C(26)	2.052(7)
Pt(2)−O(62)	2.250(5)	S(60)−O(63)	1.422(6)
S(60)−O(62)	1.433(5)	S(60)−O(61)	1.435(5)

(b) Bond Angles (deg)

C(24)−Pt(1)−C(25)	89.9(4)	C(24)−Pt(1)−C(23)	87.4(4)
C(25)−Pt(1)−C(23)	89.6(4)	C(24)−Pt(1)−N(1)	175.9(3)
C(25)−Pt(1)−N(1)	90.3(3)	C(23)−Pt(1)−N(1)	96.7(4)
C(24)−Pt(1)−N(8)	98.9(3)	C(25)−Pt(1)−N(8)	92.7(3)
C(23)−Pt(1)−N(8)	173.3(3)	N(1)−Pt(1)−N(8)	77.0(2)
C(24)−Pt(1)−O(61)	91.7(3)	C(25)−Pt(1)−O(61)	173.9(3)
C(23)−Pt(1)−O(61)	84.6(3)	N(1)−Pt(1)−O(61)	88.5(2)
N(8)−Pt(1)−O(61)	92.86(19)	C(28)−Pt(2)−C(27)	88.2(4)
C(28)−Pt(2)−C(26)	90.2(4)	C(27)−Pt(2)−C(26)	85.8(3)
C(28)−Pt(2)−N(22)	91.2(3)	C(27)−Pt(2)−N(22)	176.1(3)
C(26)−Pt(2)−N(22)	98.1(3)	C(28)−Pt(2)−N(15)	91.3(3)
C(27)−Pt(2)−N(15)	99.4(3)	C(26)−Pt(2)−N(15)	174.6(3)
N(22)−Pt(2)−N(15)	76.77(19)	C(28)−Pt(2)−O(62)	176.1(3)
C(27)−Pt(2)−O(62)	88.0(3)	C(26)−Pt(2)−O(62)	90.2(3)
N(22)−Pt(2)−O(62)	92.5(2)	N(15)−Pt(2)−O(62)	88.60(19)
S(60)−O(61)−Pt(1)	128.0(3)	S(60)−O(62)−Pt(2)	135.2(3)

Scheme 5

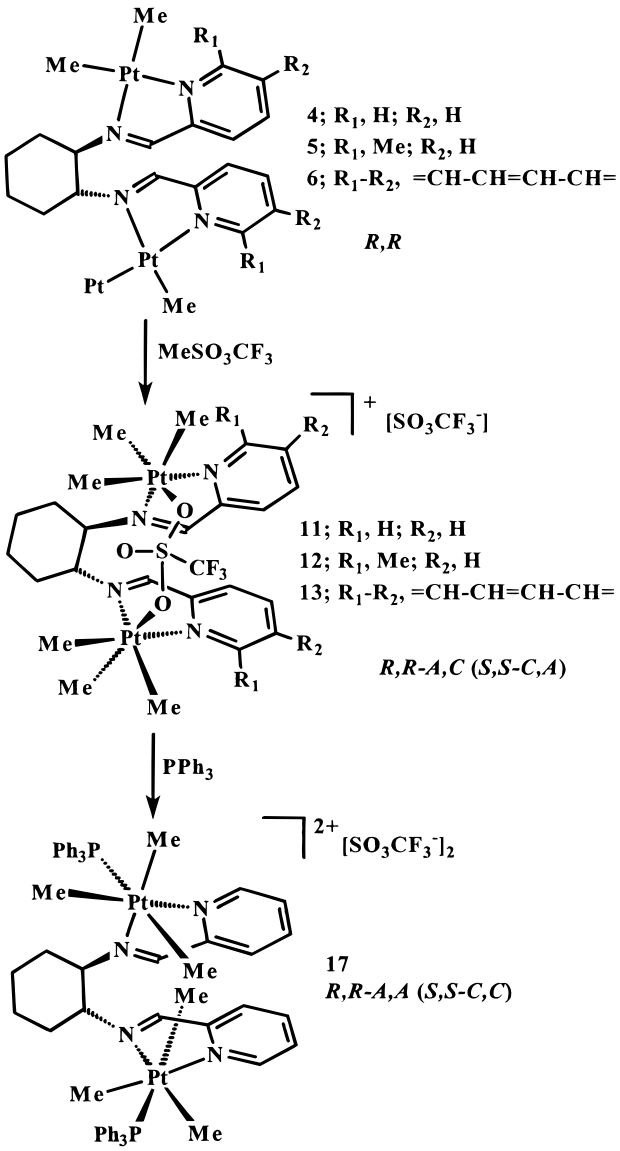

Reactions with PPh_3 and $NaBH_4$. Reaction of **10** with $NaBH_4$ gives not the platinum(IV)hydrido species as expected from recent precedents, but a covalent borohydride complex, *cis*-1,2-[C_6H_{10}{N═CH-2-C_5H_4N-($PtMe_3$)}$_2$(μ-BH_4)][O_3SCF_3], **15**.[10−11,16b,17] Although sodium borohydride ($NaBH_4$) is a very common reducing agent, chiral complexes incorporating a borohydride ion are rare,[18a] although chiral transition metal complexes

(17) (a) De Felice, V.; De Renzi, A.; Panunzi, A.; Tesauro, D. *J. Organomet. Chem.* **1995**, *488*, C13. (b) Hill, G. S.; Rendina, L. M.; Puddephatt, R. J. *Organometallics* **1995**, *14*, 4966. (c) Stahl, S. S.; Labinger, J. A.; Bercaw, J. E. *J. Am. Chem. Soc.* **1995**, *117*, 9371. (d) Hill, G. S.; Puddephatt, R. J. *J. Am. Chem. Soc.* **1996**, *118*, 8745.

(18) (a) For chiral reducing agents see: Maiti, D. K.; Bhattacharya, P. K. *Synth. Commun.* **1998**, *28* (1), 99, and references therein. (b) Yamada, T.; Ohtsuka, Y. Ikeno, T. *Chem. Lett.* **1998**, 1129.

(19) (a) Brown, M. P.; Puddephatt, R. J.; Upton, C. E. E. *J. Chem Soc., Dalton Trans.* **1974**, 2457. (b) Jawad, J. K.; Puddephatt, R. J. *J. Organomet. Chem.* **1976**, *117*, 297. (c) Jawad, J. K.; Puddephatt, R. J. *J. Chem. Soc., Dalton Trans.* **1977**, 1466. (d) Crespo, M.; Puddephatt, R. J. *Organometallics* **1987**, *6*, 2548. (e) von Zelewsky, A.; Suckling, A. P.; Stoeckli-Evans, H. *Inorg. Chem.* **1993**, *32*, 4585. (f) Achar, S.; Scott, J. D.; Puddephatt, R. J. *Polyhedron* **1996**, *15*, 2363.

Table 6. Selected Bond Distances and Angles for Complex 11

(a) Bond Distances (Å)

Pt(1)−C(24)	2.03(2)	Pt(1)−C(23)	2.03(2)
Pt(1)−C(25)	2.07(1)	Pt(1)−N(1)	2.16(1)
Pt(1)−N(8)	2.20(1)	Pt(1)−O(35)	2.26(1)
Pt(2)−C(28)	2.00(2)	Pt(2)−C(27)	2.02(1)
Pt(2)−C(26)	2.06(2)	Pt(2)−N(22)	2.18(1)
Pt(2)−N(15)	2.22(1)	Pt(2)−O(34)	2.22(1)
C(7)−N(8)	1.25(2)	N(15)−C(16)	1.25(2)

(b) Bond Angles (deg)

C(24)−Pt(1)−C(23)	86.8(8)	C(24)−Pt(1)−C(25)	88.7(8)
C(23)−Pt(1)−C(25)	89.5(8)	C(24)−Pt(1)−N(1)	97.6(7)
C(23)−Pt(1)−N(1)	174.4(6)	C(25)−Pt(1)−N(1)	94.1(6)
C(24)−Pt(1)−N(8)	174.2(6)	C(23)−Pt(1)−N(8)	99.0(6)
C(25)−Pt(1)−N(8)	91.9(6)	N(1)−Pt(1)−N(8)	76.6(5)
C(24)−Pt(1)−O(35)	86.4(6)	C(23)−Pt(1)−O(35)	91.8(7)
C(25)−Pt(1)−O(35)	174.9(6)	N(1)−Pt(1)−O(35)	85.0(5)
N(8)−Pt(1)−O(35)	92.8(4)	C(28)−Pt(2)−C(27)	89.6(8)
C(28)−Pt(2)−C(26)	91.9(9)	C(27)−Pt(2)−C(26)	84.8(8)
C(28)−Pt(2)−N(22)	89.9(7)	C(27)−Pt(2)−N(22)	98.0(7)
C(26)−Pt(2)−N(22)	176.7(7)	C(28)−Pt(2)−N(15)	91.0(7)
C(27)−Pt(2)−N(15)	173.7(7)	C(26)−Pt(2)−N(15)	101.5(6)
N(22)−Pt(2)−N(15)	75.7(5)	C(28)−Pt(2)−O(34)	178.9(7)
C(27)−Pt(2)−O(34)	89.9(7)	C(26)−Pt(2)−O(34)	87.1(7)
N(22)−Pt(2)−O(34)	91.2(4)	N(15)−Pt(2)−O(34)	89.6(4)
S(33)−O(34)−Pt(2)	137.2(7)	S(33)−O(35)−Pt(1)	124.4(6)

Table 7. Selected Bond Distances and Angles for Complex 14

(a) Bond Distances (Å)

Pt(1)−C(24)	2.02(1)	Pt(1)−C(25)	2.04(1)
Pt(1)−C(23)	2.05(2)	Pt(1)−N(1)	2.17(1)
Pt(1)−N(8)	2.18(1)	Pt(1)−O(1)	2.219(8)
C(7)−N(8)	1.27(2)	N(15)−C(16)	1.26(2)
N(15)−Pt(2)	2.19(2)	N(22)−Pt(2)	2.13(1)
C(26)−Pt(2)	2.07(2)	C(27)−Pt(2)	2.04(2)
C(28)−Pt(2)	2.02(2)	Pt(2)−O(2)	2.25(1)

(b) Bond Angles (deg)

C(24)−Pt(1)−C(25)	90.9(7)	C(24)−Pt(1)−C(23)	85.3(8)
C(25)−Pt(1)−C(23)	90.6(7)	C(24)−Pt(1)−N(1)	97.5(7)
C(25)−Pt(1)−N(1)	89.4(6)	C(23)−Pt(1)−N(1)	177.2(6)
C(24)−Pt(1)−N(8)	174.1(6)	C(25)−Pt(1)−N(8)	91.4(6)
C(23)−Pt(1)−N(8)	100.1(6)	N(1)−Pt(1)−N(8)	77.0(5)
C(24)−Pt(1)−O(1)	90.9(5)	C(25)−Pt(1)−O(1)	177.5(6)
C(23)−Pt(1)−O(1)	91.3(6)	N(1)−Pt(1)−O(1)	88.6(4)
N(8)−Pt(1)−O(1)	86.7(3)	N(8)−C(7)−C(6)	119(1)
C(7)−N(8)−C(9)	109(2)	C(7)−N(8)−Pt(1)	113.2(9)
C(16)−N(15)−Pt(2)	111(1)	C(28)−Pt(2)−C(27)	90(1)
C(28)−Pt(2)−C(26)	88.5(8)	C(27)−Pt(2)−C(26)	87(1)
C(28)−Pt(2)−N(22)	90.2(6)	C(27)−Pt(2)−N(22)	97.5(8)
C(26)−Pt(2)−N(22)	176(1)	C(28)−Pt(2)−N(15)	91.9(7)
C(27)−Pt(2)−N(15)	173.7(9)	C(26)−Pt(2)−N(15)	99(1)
N(22)−Pt(2)−N(15)	76.5(7)	C(28)−Pt(2)−O(2)	179.4(6)
C(27)−Pt(2)−O(2)	89.9(7)	C(26)−Pt(2)−O(2)	92.1(7)
N(22)−Pt(2)−O(2)	89.2(4)	N(15)−Pt(2)−O(2)	88.0(5)

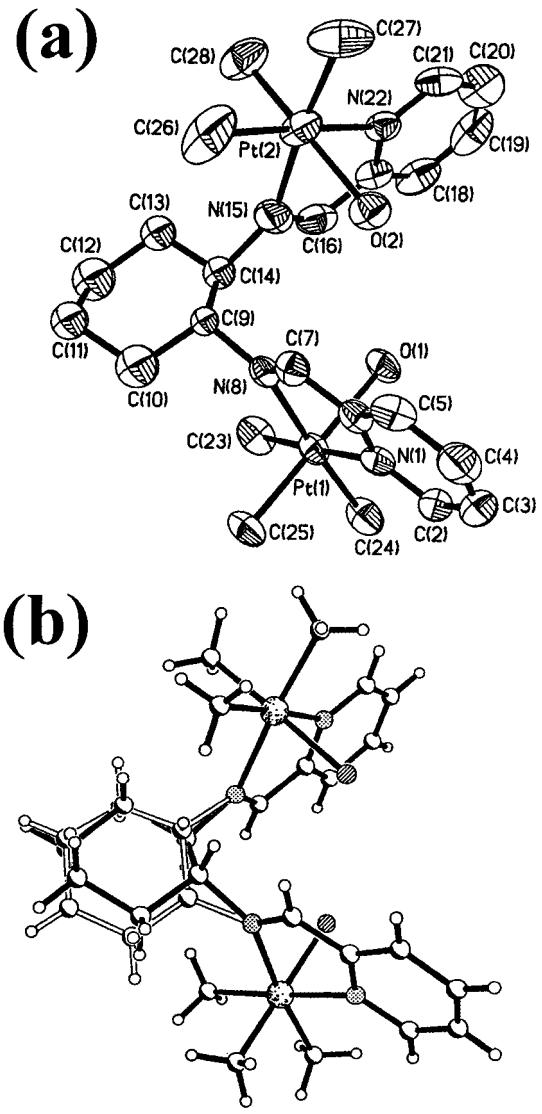

Figure 8. View of the structure of the dicationic diaqua complex **14**. (a) The overall structure with *A,A* configuration at platinum. (b) The disorder, showing superimposed *R,R-C,C* and *S,S-C,C* diastereomers.

have been used as reduction catalysts in the presence of premodified borohydride.[18b] In the ^{1}H NMR of **15**, the borohydride ligand gives a single broad resonance at $\delta = -3.0$, with no resolved coupling to platinum, and no change was observed in the spectrum at −80 °C. The ^{11}B NMR spectrum contains a broad singlet at $\delta = -22.4$.[10,11] The infrared spectrum has a very strong, broad absorption at 1981 cm^{-1}, which rules out an ionic tetrahydroborate complex and is consistent with the presence of a covalently bound borohydride ligand.[10,11] The ^{1}H NMR spectrum indicates that the complex is C_s symmetric, with three methylplatinum(IV) resonances and one imine signal. The methyl group *trans* to the BH_4 ligand is at $\delta = 0.57$ with ^2J(PtH) = 73 Hz. The large decrease in the ^2J(PtH) value relative to **10** is consistent with the replacement of triflate by the bridging borohydride ligand, which has a stronger *trans*-influence. There is a single resonance in the ^{19}F NMR spectrum for the free triflate anion. The BH_4 ligand bridges the two platinum(IV) centers, as was confirmed by an X-ray crystal structure determination (see below). Similar reactions with $NaBH_4$ carried out for complexes **11**−**13** indicated formation of similar compounds, having the same stereochemistry as the triflate precursor, but they could not be isolated in pure form.

Recrystallization of **15** from CH_2Cl_2/pentane occurred with partial decomposition, and the crystals obtained were found to be a 1:1 mixture of **15** and complex **16**, in which borohydride is replaced by chloride. Fortunately, the asymmetric unit contained distinct molecules of **15** and **16** rather than a disordered mixture. The structures of complexes **15** and **16** are given in Figure 9, with selected bond distances and angles in Table 8. The borohydride ligand was not accurately located in **15**, but the structure does establish the mode of coordination for the BH_4 as well as the absolute stereochemistry for complex **15**. Each of the platinum atoms is bonded to a

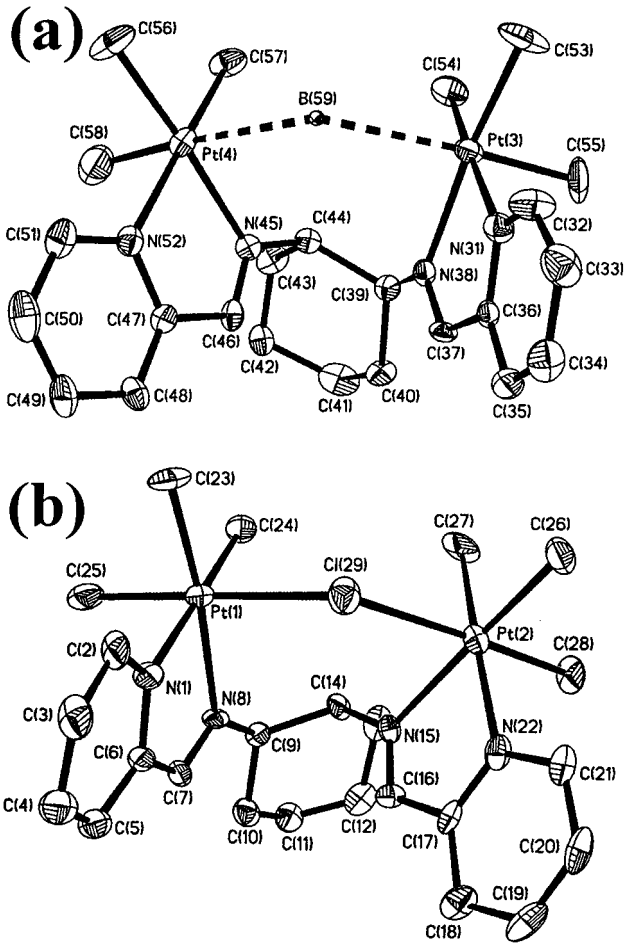

Figure 9. Views of the structures of (a) the cationic borohydride complex **15** and (b) the corresponding bridging chloro complex **16**, each in the *R,S-A,C* isomeric form with approximate C_s symmetry.

Table 8. Selected Bond Distances and Angles for Complexes 15/16

(a) Bond Distances (Å)

Pt(3)−C(55)	2.02(2)	Pt(3)−C(54)	2.06(1)
Pt(3)−C(53)	2.07(2)	Pt(3)−N(31)	2.14(1)
Pt(3)−N(38)	2.19(1)	C(37)−N(38)	1.24(2)
N(45)−C(46)	1.30(2)	N(45)−Pt(4)	2.15(1)
N(52)−Pt(4)	2.16(1)	Pt(4)−C(58)	2.01(3)
Pt(4)−C(56)	2.05(2)	Pt(4)−C(57)	2.06(1)
Pt(4)−B(59)	2.61(1)	Pt(3)−B(59)	2.72(2)
Pt(1)−C(24)	2.04(1)	Pt(1)−C(23)	2.05(2)
Pt(1)−C(25)	2.07(2)	Pt(1)−N(1)	2.14(1)
Pt(1)−N(8)	2.17(1)	Pt(1)−Cl(29)	2.598(5)
Pt(2)−C(27)	2.04(2)	Pt(2)−C(28)	2.06(2)
Pt(2)−C(26)	2.06(2)	Pt(2)−N(22)	2.15(1)
Pt(2)−N(15)	2.21(1)	Pt(2)−Cl(29)	2.556(6)

(b) Bond Angles (deg)

C(55)−Pt(3)−C(54)	84.7(8)	C(55)−Pt(3)−C(53)	90(1)
C(54)−Pt(3)−C(53)	86.1(10)	C(55)−Pt(3)−N(31)	91.1(7)
C(54)−Pt(3)−N(31)	175.5(6)	C(53)−Pt(3)−N(31)	95.4(8)
C(55)−Pt(3)−N(38)	88.1(9)	C(54)−Pt(3)−N(38)	102.0(7)
C(53)−Pt(3)−N(38)	171.3(8)	N(31)−Pt(3)−N(38)	76.2(5)
C(58)−Pt(4)−C(56)	89.0(1)	C(58)−Pt(4)−C(57)	88.0(1)
C(56)−Pt(4)−C(57)	85.4(8)	C(58)−Pt(4)−N(45)	92.6(9)
C(56)−Pt(4)−N(45)	174.3(7)	C(57)−Pt(4)−N(45)	100.1(6)
C(58)−Pt(4)−N(52)	90.1(8)	C(56)−Pt(4)−N(52)	97.6(8)
C(57)−Pt(4)−N(52)	176.4(8)	N(45)−Pt(4)−N(52)	77.0(4)
C(58)−Pt(4)−B(59)	174.1(7)	C(56)−Pt(4)−B(59)	96.0(9)
C(57)−Pt(4)−B(59)	89.9(8)	N(45)−Pt(4)−B(59)	82.5(5)
N(52)−Pt(4)−B(59)	91.8(4)		

bridging hydride of the tetrahydroborate ligand which is part of a Pt−H_B−B−H_B−Pt intramolecular bridge, and the boron atom lies near the center of the Pt···Pt vector. The μ-BH_4 group bridges the same two diastereotopic faces of the (N−N)$PtMe_2$ meridia as in complexes **7b** and **10**. Hence, the absolute configuration remains *R,S-A,C* (the BH_4 ligand is given highest priority in assigning the absolute configuration of **15** to demonstrate the common stereochemistries of complexes **7b**, **10**, **15**, and **16**). The BH_4 is smaller than the triflate ligand, and a corresponding decrease in the platinum atom internuclear separation is observed in the structure for **15**, with d(Pt−Pt) = 4.61 Å. The chloride derivative **16** has a similar structure but has a slightly shorter d(Pt−Pt) = 4.52 Å.

The reaction of **11** with PPh_3 gave a new C_2-symmetric complex. The pattern of six methylplatinum(IV) and two imine resonances due to **11** was replaced by a C_2-symmetric pattern of three methylplatinum(IV) signals and a single imine signal for complex **17**. Apparently, replacement of the triflate ligand in **11** with a ligand that cannot bridge the two platinum atoms, in this case a bulky PPh_3 group, favors the formation of diastereomerically pure C_2-symmetric product. The similarities in the ^{1}H NMR data of **17** and **8b** suggest, but do not prove, that complex **17** has the same stereochemistry as **8b**.

Discussion

In most cases, oxidative addition of primary alkyl halides to square-planar platinum(II) occurs by the polar S_N2 mechanism in which *trans* stereochemistry is observed for the kinetic product, although subsequent isomerization can occur.[14d,19] The nucleophilic attack is expected to occur from the least hindered face of the square plane.[4] Thus, for a binuclear complex, attack might be expected at opposite sides of each platinum(II) center, resulting in *anti* stereochemistry, as observed in the initial formation of complexes **7a** and **8a**.[8] Since the presumed Pt(II)−Pt(IV) mixed oxidation state intermediates were not observed, no information regarding the stereoselectivity of the initial oxidative addition was obtained. In this work, the isolated products are generally those formed by thermodynamic control, although the kinetic products could sometimes be identified by their NMR spectra and even isolated in favorable cases. The stereoselectivity of oxidative addition to diplatinum(II) substrates **3** and **4** can be understood in terms of two factors. First, there is a natural tendency to minimize the steric hindrance, which may involve the ligands on each platinum(IV) center and the bulky cyclohexyl group. Second, there is a propensity to form an intramolecular $Pt_2(\mu$-X) bridge between two platinum(IV) centers.

Consider first the oxidative addition of CH_3I or $MeSO_3CF_3$ to complex **3**, containing the ligand derived from *cis*-diaminocyclohexane. The thermodynamically favored products **7b** and **10b** have the *syn* arrangement for the axial methyl ligands, with absolute configuration *R,S-A,C*, and there is always a bridging ligand X = I or O_3SCF_3 connecting the two platinum(IV) centers. It is clear then that bridge formation is a facile process with the *cis*-ligand complexes. The absolute configuration *R,S-A,C* is favored because it maximizes the distance between methylplatinum(IV) ligands and the cyclohexane ring. Molecular modeling of the *R,S-C,A* diastere-

Table 9. Molecular Mechanics Calculations of Relative Energies (kcal/mol) for Isomers of Complexes 7−11[a]

cis-Ligand Isomers

C_s-symmetric	asymmetric	relative energy
	7a (*R,S-A,A*)	33.92
7b (*R,S-A,C*)-*b*[b,c]		**33.83**
7c (*R,S-C,A*)-*b*		40.45
	7d (*R,S-A,A*)-*b*	36.16
7e (*R,S-A,C*)		31.57
7f (*R,S-C,A*)		32.63
	10a (*R,S-A,A*)	36.00
10b (*R,S-A,C*)-*b*		**34.52**
10c (*R,S-C,A*)-*b*		44.95
	10d (*R,S-A,A*)-*b*	38.43
10e (*R,S-A,C*)		33.09
10f (*R,S-C,A*)		33.00

trans-Ligand Isomers

C_2-symmetric	asymmetric	relative energy
8a (*S,S-A,A*)		29.28
8b (*S,S-C,C*)		**27.33**
8c (*S,S-A,A*)-*b*		40.51
8d (*S,S-C,C*)-*b*		30.95
	8e (*S,S-C,A*)	31.65
	8f (*S,S-C,A*)-*b*	33.24
11a (*S,S-A,A*)		31.70
11b (*S,S-C,C*)		30.46
11c (*S,S-A,A*)-*b*		38.52
11d (*S,S-C,C*)-*b*		39.60
	11e (*S,S-C,A*)	31.17
	11f (*S,S-C,A*)-*b*	**33.36**

[a] Table 9 includes all potential stereoisomers, while only those observed are shown in the Schemes. [b] The *b* denotes a diplatinum complex that contains an intramolecular bridge, X (X = I, SO_3CF_3). [c] The major product is given in bold face.

omer (Table 9) shows that the methyl ligands on each platinum atom are directed toward each other and the cyclohexyl ring, increasing the steric interactions between these groups.[15] For the *R,S-A,A* diastereomer the methyl ligands of one platinum center are in close steric contact with the cyclohexane ring. Molecular mechanics calculations show higher relative energies for these diastereomers that are not observed: compare **7b**, **10b**(*R,S-A,C*)-*b* to **7c**, **10c**(*R,S-C,A*)-*b* and **7d**, **10d**(*R,S-A,A*)-*b* (Table 9, the designation -*b* indicates an X-bridged structure).[15]

Consider next the oxidative addition of CH_3I or $MeSO_3CF_3$ to complex **4**, with the ligand derived from *trans*-diaminocyclohexane. In this case, the thermodynamically favored product **8b** for CH_3I addition contains no intramolecular bridging iodide ligand, although isomers containing bridging iodide are observed as intermediates. Thus, while the formation of the iodo bridge is possible, it does not control product formation as it does with the *cis*-ligand complexes described above, probably because the conformation with platinum atoms close enough to allow iodide bridging is strained. The lower stereoselectivity observed may also be the result of smaller steric interactions in the *trans*-ligand system, in which the platinum centers can be well separated. The stereoselective isomerization to **8b** is presumably to minimize steric interactions in the diplatinum(IV) complex, and this is consistent with the predictions of the molecular mechanics calculations (Table 9).[15]

The improved stereoselectivity on formation of complexes **11**−**13** is suggested to be the result of the very different sizes of the iodide and triflate ligands, with the larger triflate better able to bridge between two platinum atoms in the *trans*-ligand complexes. Thus, for oxidative addition of $MeOSO_2CF_3$ the bridged isomers are favored, resulting in a different stereochemistry for complexes **11**−**13** compared to **8**. If the bridge is broken, as in the reaction of **11** with PPh_3 to give complex **17**, the stereochemistry reverts to being analogous to **8b.** The preference for isomer **11f** over C_2-symmetric species such as **11c** or **11d** is presumably because the triflate ligand fits best into the bridging position in **11f** while minimizing steric contacts. This is supported by the molecular mechanics calculations (Table 9).[15] The observed diastereomer **11f**(*S,S-C,A*)-*b* has the CF_3 group near the center of the cavity pointed away from the platinum atoms and the methyl ligands, where steric effects are lower than is possible in **11c** or **11d**.

Displacement of the labile triflate ligand in chiral platinum(IV) complexes **10**−**13** can give rise to diastereomerically pure PPh_3 and μ-BH_4 complexes. When the ligand is capable of bridging two transition metals, as in the case of BH_4 or Cl, the stereochemistry of the triflate substrate was maintained. If instead a bulky ligand such as PPh_3 is used, the stereochemistry is different from that of the tiflate precursor, thus supporting the hypothesis that the observed stereochemistry depends on whether the introduced ligand can bridge the platinum centers. When the triflate ligand is displaced by less bulky water ligands, the stereochemistry is again different from the triflate precursor, but two diastereomers are formed in equal amounts. Easy formation of more than one diastereomer is attributed to the very labile nature of the aqua ligand. Both the PPh_3 and the aqua ligands produce a C_2-symmetric product. The converse was observed in the reaction of $AgOCOCF_3$ to complex **8b**, in which the removal of a terminal iodide ligand leads to formation of an intramolecular iodo bridge, with change in absolute configuration from *S,S-C,C* in **8b** to *S,S-C,A* in **8f**.

Conclusions

These reactions show that high degrees of diastereoselectivity are possible for the intermolecular oxidative addition of methyl iodide and methyl triflate to chiral diplatinum(II) complexes. We have shown that the stereochemistry of the diplatinum(IV) products is determined by steric interactions, including interactions with the supporting chiral ligands (which are derived from *cis*- or *trans*-1,2-diaminocyclohexane) and the nature of the added ligands (from MeI or $MeOSO_2CF_3$) in large part by affecting the degree to which the platinum nuclei can cooperate with one another to form a $Pt_2(\mu$-X) bridge. The observed stereoselectivity was highest when a $Pt_2(\mu$-X) bridge could be formed. Since the oxidative addition of methyl triflate gives diastereomerically pure platinum(IV) complexes, the synthesis of additional platinum(IV) complexes as single diastereomers was possible by displacement of the triflate ligand. As with the oxidative addition reactions, the stereochemistry of the chiral diplatinum(IV) complexes was controlled by choice of ligand and could be changed or maintained in the displacement products.

Experimental Section

General Procedures. All reactions were carried out under an N_2 atmosphere using standard Schlenk techniques. NMR

spectra were recorded using a Varian Gemini spectrometer (^{1}H at 300.10 MHz, ^{11}B at 64.17 MHz, and ^{19}F at 282.32 MHz). Chemical shifts are given in ppm with respect to TMS (^{1}H), $BF_3{\cdot}Et_2O$ (^{11}B), or $CFCl_3$ (^{19}F). The ^{11}B and ^{19}F chemical shifts are referenced to $BF_3{\cdot}Et_2O$ or $CFCl_3$, respectively, contained in a coaxial insert. The IR spectrum of **15** was recorded as a Nujol mull using a Perkin-Elmer 2000 FT-IR instrument. The complexes $[PtMe_2(\mu\text{-}SMe_2)]_2$,[20] *cis*-1,2-$[C_6H_{10}\{N{=}CH\text{-}2\text{-}C_5H_4N\text{-}(PtMe_2)\}_2]$, **3**, and racemic *trans*-1,2-$[C_6H_{10}\{N{=}CH\text{-}2\text{-}C_5H_4N\text{-}(PtMe_2)\}_2]$, **4**, were prepared as reported in the literature.[5]

Synthesis of Ligands. To a solution of racemic (*R*,*R*/*S*,*S*) *trans*-1,2-diaminocyclohexane (0.49 mL) in diethyl ether (40 mL) was added 6-methyl-2-pyridinecarboxaldehyde (0.99 g). Excess $MgSO_4$ was added to the reaction mixture to remove product water. The solution was stirred for 15 h at room temperature and filtered to remove the $MgSO_4$. The solution was then concentrated under reduced pressure causing a white precipitate to form. The yellow supernatant was removed and the white solid was washed with cold diethyl ether (3 × 5 mL) to give pure racemic ***trans*-1,2-$C_6H_{10}(N{=}CH\text{-}2\text{-}MeC_5H_3N)_2$, 2b** ($MeC_5H_3N$ = 6-methylpyridyl). Yield = 0.83 g (64%). ^{1}H NMR ($CDCl_3$): δ 1.48 [m, 2H]; 1.71 [m, 6H]; 2.50 [s, 6H, 6-Me]; 3.48 [m, 2H, NCH]; 7.05 [t, 2H]; 7.49 [d, 2H]; 7.70 [d, 2H]; 8.27 [s, 2H, N=CH]. Similarly prepared but from 2-quinolinecarboxaldehyde was ***trans*-1,2-$C_6H_{10}(N{=}CH\text{-}2\text{-}C_9H_6N)_2$, 2c** ($C_9H_6N$ = quinolyl). Yield = 40%. ^{1}H NMR ($CDCl_3$): δ 1.53 [m, 2H]; 1.88 [m, 6H]; 3.63 [m, 2H, NCH]; 7.46 [m, 2H]; 7.63 [m, 2H]; 7.71 [m, 2H]; 8.01 [d, 2H]; 8.05 [s, 4H]; 8.49 [s, 2H, N=CH].

***R*,*R*/*S*,*S*-*trans*-1,2-$[C_6H_{10}\{N{=}CH\text{-}2\text{-}MeC_5H_3N\text{-}(PtMe_2)\}_2]$, 5.** To a suspension of $[PtMe_2(\mu\text{-}SMe_2)]_2$ (0.075 g, 0.130 mmol) in diethyl ether (10 mL) was added racemic *trans*-1,2-$C_6H_{10}(N{=}CH\text{-}2\text{-}MeC_5H_3N)_2$, **2a** (0.042 g, 0.261 mmol), to give a red solution, from which a dark red precipitate began to separate. The mixture was stirred for 15 h at room temperature, the volume reduced to 3 mL under reduced pressure, and the red solid isolated by filtration. The product was washed with several portions of cold diethyl ether (3 × 5 mL) and pentane (3 × 10 mL). Yield = 0.089 g (88%). ^{1}H NMR (CD_2Cl_2): δ 1.50 [s, 6H, ^2J(PtH) = 90 Hz, Pt−Me]; 1.80 [s, 6H, ^2J(PtH) = 84 Hz, Pt−Me]; 1.57 [m, 2H, Cy]; 1.77 [br s, 2H, Cy]; 1.93 [br m, 2H, Cy]; 2.56 [br m, 2H, Cy]; 2.73 [s, 6H, 6-Me]; 4.85 [m, 2H, NCH]; 7.40 [d, 2H]; 7.57 [d, 2H]; 7.84 [t, 2H]; 9.56 [s, 2H, ^3J(PtH) = 33 Hz, N=CH].

The complex ***R*,*R*/*S*,*S*-*trans*-1,2-$[C_6H_{10}\{N{=}CH\text{-}2\text{-}C_9H_6N\text{-}(PtMe_2)\}_2]$, 6**, was similarly prepared but from racemic *trans*-1,2-$C_6H_{10}(N{=}CH\text{-}2\text{-}C_9H_6N)_2$, **2b.** Yield = 0.08 g (69%). Anal. Calcd for $C_{30}H_{36}N_4Pt_2$: C, 42.8; H, 4.3; N, 6.7. Found: C, 42.9; H, 4.4; N, 6.3. ^{1}H NMR (CD_2Cl_2): δ 1.43 [s, 6H, ^2J(PtH) = 90 Hz, Pt−Me]; 1.53 [s, 6H, ^2J(PtH) = 84 Hz, Pt−Me]; ca. 1.62−1.70 [br m, 3H, Cy]; 2.0 [br m, 3H, Cy]; 3.68 [br m, 2H, Cy]; 5.08 [m, 2H, NCH]; 7.46−7.93 [m, 8H]; 8.41 [d, 2H]; 8.86 [br d, 2H]; 9.96 [s, 2H, ^3J(PtH) = 35 Hz, N=CH].

***cis*-1,2-$[C_6H_{10}\{N{=}CH\text{-}2\text{-}C_5H_4N(PtMe_3I)\}_2]$, 7a.** An NMR tube was charged with a concentrated solution of complex **3** in CD_2Cl_2 and placed in a −78 °C bath. To this was added excess MeI, and after 5 min the ^{1}H NMR spectrum was recorded at −78 °C. ^{1}H NMR (CD_2Cl_2): δ 0.59 [s, 3H, ^2J(PtH) = 72 Hz, Pt−Me]; 0.80 [s, 3H, ^2J(PtH) = 72 Hz, Pt−Me]; 1.41 [s, 3H, ^2J(PtH) = 71 Hz, Pt−Me]; 1.50 [s, 3H, ^2J(PtH) = 71 Hz, Pt−Me]; 1.51 [s, 3H, ^2J(PtH) = 71 Hz, Pt−Me]; 1.54 [s, 3H, ^2J(PtH) = 71 Hz, Pt−Me]; 2.61 [br m, 1H, Cy]; 3.14 [br m, 1H, Cy]; 4.29 [br m, 1H, NCH]; 5.26 [br s, 1H, NCH]; 7.60 [m, 1H]; 7.68 [m, 1H]; 7.94 [t d, 1H]; 8.07 [m, 2H]; 8.62 [d, 1H]; 8.89 [m, 2H]; 9.32 [s, 1H, ^3J(PtH) = 28 Hz, N=CH]; 9.79 [s, 1H, ^3J(PtH) = 27 Hz, N=CH].

***cis*-1,2-$[C_6H_{10}\{N{=}CH\text{-}2\text{-}C_5H_4N(PtMe_3)\}_2(\mu\text{-}I)]$I, 7b.** To a red solution of complex **3** (0.07 g, 0.094 mmol) in THF (10 mL) was added MeI (0.29 mL, 4.7 mmol), turning the solution bright orange. Stirring was continued for 15 h to give a pale yellow solution with some yellow precipitate. The solution was concentrated under reduced pressure, and pentane (40 mL) was added to complete the precipitation of a yellow powder. The product was isolated by filtration and washed with pentane (3 × 20 mL). Yield = 0.07 g (72%). Anal. Calcd for $C_{24}H_{38}N_4I_2Pt_2$: C, 28.1; H, 3.7; N, 5.5. Found: C, 28.3; H, 4.0; N, 5.3. ^{1}H NMR (CD_2Cl_2): δ 0.72 [s, 6H, ^2J(PtH) = 76 Hz, Pt−Me]; 1.27 [s, 6H, ^2J(PtH) = 68 Hz, Pt−Me]; 1.39 [s, 6H, ^2J(PtH) = 69 Hz, Pt−Me]; 1.72 [br m, 2H, Cy]; 1.91 [br m, 2H, Cy]; 2.15 [br m, 2H, Cy]; 2.82 [br m, 2H, Cy]; 5.03 [br s, 2H, NCH]; 7.56 [m, 2H]; 8.03 [t d, 2H]; 8.61 [d, 2H]; 9.26 [d, 2H]; 10.14 [s, 2H, ^3J(PtH) = 32 Hz, N=CH].

***R*,*R*/*S*,*S*-*trans*-1,2-$[C_6H_{10}\{N{=}CH\text{-}2\text{-}C_5H_4N(PtMe_3I)\}_2]$, 8b/8e, and *R*,*R*/*S*,S-*trans*-1,2-$[C_6H_{10}\{N{=}CH\text{-}2\text{-}C_5H_4N(PtMe_3)\}_2(\mu\text{-}I)]$I, 8c/8d**, were similarly prepared as a mixture from complex **4**. Yield = 81%. Anal. Calcd for $C_{24}H_{38}N_4I_2Pt_2{\cdot}0.25C_4H_8O$: C, 28.8; H, 3.9; N, 5.4. Found: C, 28.8; H, 3.8; N, 5.4. Alternatively, an NMR tube was charged with a concentrated solution of complex **4** in CD_2Cl_2, and excess MeI was added. Complexes **8a**−**e** were identified in situ. Complex **8b** could also be isolated as a precipitate from a concentrated CH_2Cl_2 solution of a mixture of **8b**−**e**. Washing the precipitate with small portions of cold CH_2Cl_2 gave pure **8b**. ^{1}H NMR (CD_2Cl_2): **8a**, δ = 0.8 [br s, 6H, ^2J(PtH) = 71 Hz, Pt−Me]; 1.58 [br s, 6H, ^2J(PtH) = 71 Hz, Pt−Me]; 1.58 [br s, 6H, ^2J(PtH) = 71 Hz, Pt−Me]; 10.10 [br s, 2H, ^3J(PtH) = 25 Hz, N=CH]; **8b**, δ 0.72 [s, 6H, ^2J(PtH) = 73 Hz, Pt−Me]; 1.45 [s, 6H, ^2J(PtH) = 70 Hz, Pt−Me]; ca.1.24−1.66 [br m, 4H, Cy]; 1.52 [s, 6H, ^2J(PtH) = 70 Hz, Pt−Me]; 1.97 [br m, 2H, Cy]; 2.62 [br d, 2H, Cy]; 4.86 [m, 2H, NCH]; 7.58 [t, 2H]; 7.95 [t, 2H]; 8.62 [d, 2H]; 8.81 [d, 2H]; 9.81 [s, 2H, ^3J(PtH) = 30 Hz, N=CH]; **8c/8d**, δ 0.57 [s, 6H, ^2J(PtH) = 72 Hz, Pt−Me]; 0.69 [s, 6H, ^2J(PtH) = 76 Hz, Pt−Me]; 1.44 [s, 6H, ^2J(PtH) = 70 Hz, Pt−Me]; 1.49 [s, 6H, ^2J(PtH) = 70 Hz, Pt−Me]; 1.50 [s, 6H, ^2J(PtH) = 71 Hz, Pt−Me]; 1.52 [s, 6H, ^2J(PtH) = 70 Hz, Pt−Me]; 8.73 [s, 2H, ^3J(PtH) = 31 Hz, N=CH]; 9.55 [s, 2H, ^3J(PtH) = 29 Hz, N=CH]; **8e**, δ 0.74 [s, 3H, ^2J(PtH) = 76 Hz, Pt−Me]; 0.86 [s, 3H, ^2J(PtH) = 75 Hz, Pt−Me]; 1.21 [s, 3H, ^2J(PtH) = 68 Hz, Pt−Me]; 1.40 [s, 3H, ^2J(PtH) = 70 Hz, Pt−Me]; 1.43 [s, 3H, ^2J(PtH) = 70 Hz, Pt−Me]; 1.65 [s, 3H, ^2J(PtH) = 71 Hz, Pt−Me]; 10.39 [s, 1H, ^3J(PtH) = 34 Hz, N=CH]; 10.70 [s, 1H, ^3J(PtH) = 27 Hz, N=CH].

***R*,*R*/*S*,*S*-*trans*-1,2-$[C_6H_{10}\{N{=}CH\text{-}2\text{-}C_5H_4N(PtMe_3)\}_2(\mu\text{-}I)]$-$[CF_3CO_2]$, 8f.** To an NMR tube charged with a CD_2Cl_2 solution of complex **8b** (1.25 mg, 0.012 mmol) was added $AgOCOCF_3$ (3 mg, 0.24 mmol) to precipitate a white solid. The solution was filtered to remove AgI, and the ^{1}H NMR spectrum was recorded. ^{1}H NMR (CD_2Cl_2): δ 0.75 [s, 3H, ^2J(PtH) = 76 Hz, Pt−Me]; 0.87 [s, 3H, ^2J(PtH) = 75 Hz, Pt−Me]; 1.20 [s, 3H, ^2J(PtH) = 68 Hz, Pt−Me]; 1.40 [s, 3H, ^2J(PtH) = 70 Hz, Pt−Me]; 1.43 [s, 3H, ^2J(PtH) = 70 Hz, Pt−Me]; 1.62 [br m, 2H, Cy]; 1.66 [s, 3H, ^2J(PtH) = 71 Hz, Pt−Me]; 1.99 [br m, 2H, Cy]; 2.10−2.33 [br m, 4H, Cy]; 5.12 [m, 2H, NCH]; 7.56 [m, 2H]; 8.01 [m, 2H]; 8.37 [d m, 1H]; 8.57 [d m, 1H]; 8.63 [m, 2H]; 10.09 [s, 1H, ^3J(PtH) = 34 Hz, N=CH]; 10.15 [s, 1H, ^3J(PtH) = 27 Hz, N=CH].

***R*,*R*/*S*,*S*-*trans*-1,2-$[C_6H_{10}\{N{=}CH\text{-}2\text{-}C_9H_6N(PtMe_3I)\}_2]$, 9b**, was prepared by adding an excess of MeI to a CD_2Cl_2 solution of complex **6**. ^{1}H NMR (CD_2Cl_2): δ 0.58 [s, 6H, ^2J(PtH) = 70 Hz, Pt−Me]; 1.64 [s, 6H, ^2J(PtH) = 70 Hz, Pt−Me]; ca. 1.24−1.82 [br m, 4H, Cy]; 1.72 [s, 6H, ^2J(PtH) = 72 Hz, Pt−Me]; 2.02 [br m, 2H, Cy]; 2.62 [br d, 2H, Cy]; 5.10 [m, 2H, NCH]; 7.65 [m, 2H]; 7.78−7.88 [m, 4H]; 8.32 [d, 2H]; 8.51 [d, 2H]; 8.62 [d, 2H]; 10.10 [s, 2H, ^3J(PtH) = 31 Hz, N=CH].

***cis*-1,2-$[C_6H_{10}\{N{=}CH\text{-}2\text{-}C_5H_4N(PtMe_3)\}_2(\mu\text{-}OSO_2CF_3)]$-$[SO_3CF_3]$, 10.** To a red solution of **3** (0.110 g, 0.148 mmol) in CH_2Cl_2 (10 mL) was added $MeSO_3CF_3$ (0.24 g, 1.48 mmol), turning the solution bright orange. The solution was stirred for 15 h, during which time it turned pale yellow. Evaporation

(20) Hill, G. S.; Irwin, M. J.; Levy, C. J.; Rendina, L. M.; Puddephatt, R. J. *Inorg. Synth.* **1998**, *32*, 149.

of the solvent gave a pale yellow solid, which was dried under reduced pressure. Yield = 0.15 g (95%). Anal. Calcd for $C_{26}H_{38}N_4O_6F_6S_2Pt_2$: C, 29.2; H, 3.6; N, 5.2. Found: C, 28.8; H, 3.5; N, 5.1. ^{1}H NMR ($CDCl_3$): δ 0.74 [s, 6H, ^2J(PtH) = 84 Hz, Pt−Me]; 1.17 [s, 6H, ^2J(PtH) = 66 Hz, Pt−Me]; 1.18 [s, 6H, ^2J(PtH) = 66 Hz, Pt−Me]; 1.72 [br m, 4H, Cy]; 2.08 [br m, 2H, Cy]; 2.65 [br, m, 2H, Cy]; 4.89 [br s, 2H, NCH]; 7.63 [m, 2H]; 8.11 [t d, 2H]; 8.60 [d, 2H]; 8.76 [d, 2H]; 9.75 [s, 2H, ^3J(PtH) = 30 Hz, N=CH]. ^{19}F NMR (CD_2Cl_2): δ −78.5 (s), −78.6 (s).

***R,R/S,S-trans*-1,2-[C_6H_{10}{N=CH-2-C_5H_4N(PtMe$_3$)}$_2$(μ-OSO$_2$CF$_3$)][SO$_3$CF$_3$], 11.** To a red suspension of complex **4** (0.11 g, 0.148 mmol) in diethyl ether (10 mL) was added $MeSO_3CF_3$ (0.24 g, 1.48 mmol). The mixture was stirred for 15 h, producing a yellow suspension. The precipitate was isolated by filtration and washed with diethyl ether (3 × 10 mL) to give a pale yellow solid. Yield = 0.12 g (76%). Anal. Calcd for $C_{26}H_{38}N_4O_6F_6S_2Pt_2$: C, 29.2; H, 3.6; N, 5.2. Found: C, 29.1; H, 3.3; N, 5.0. ^{1}H NMR (CD_2Cl_2): δ 0.90 [s, 6H, ^2J(PtH) = 86 Hz, coincident Pt−Me's]; 1.20 [s, 3H, ^2J(PtH) = 66 Hz, Pt−Me]; 1.27 [s, 6H, ^2J(PtH) = 67 Hz, coincident Pt−Me's]; 1.48 [s, 3H, ^2J(PtH) = 66 Hz, Pt−Me]; 1.62 [br m, 3H, Cy]; 1.98 [br m, 2H, Cy]; 2.12 [br m, 1H]; 2.27 [br m, 1H]; 2.44 [br d, 1H]; 5.08 [br m, 2H, NCH]; 7.68 [m, 2H]; 8.14 [m, 2H]; 8.30 [d, 1H]; 8.64 [m, 3H]; 9.75 [s, 1H, ^3J(PtH) = 30 Hz, N=CH]; 9.83 [s, 1H, ^3J(PtH) = 27 Hz, N=CH]. ^{19}F NMR ($CDCl_3$): δ = −78.7 (s); −78.9 (s).

Complexes **12** and **13** were similarly prepared from complexes **5** and **6**, respectively.

***R,R/S,S-trans*-1,2-[C_6H_{10}{N=CH-2-C_6H_6N(PtMe$_3$)}$_2$(μ-OSO$_2$CF$_3$)][SO$_3$CF$_3$], 12.** Yield = 56%. Anal. Calcd for $C_{28}H_{42}N_4O_6F_6S_2Pt_2$: C, 30.6; H, 3.9; N, 5.1. Found: C, 30.7; H, 3.8; N, 4.9. ^{1}H NMR (CD_2Cl_2): δ 0.94 [s, 3 H, ^2J(PtH) = 84 Hz, Pt−Me]; 1.04 [s, 3H, ^2J(PtH) = 84 Hz, Pt−Me]; 1.31 [s, 3H, ^2J(PtH) = 66 Hz, Pt−Me]; 1.39 [s, 3 H, ^2J(PtH) = 69 Hz, Pt−Me]; 1.42 [s, 3 H, ^2J(PtH) = 69 Hz, Pt−Me]; ca. 1.44−1.63 [br m, 3H, Cy]; 1.64 [s, 3H, ^2J(PtH) = 68 Hz, Pt−Me]; 1.96 [br m, 2H, Cy]; 2.12 [br m, 1H, Cy]; 2.22−2.43 [br m, 2H, Cy]; 2.73 [s, 6H, coincident 6-Me's]; 5.08 [m, 2H, NCH]; 7.43 [t, 2H]; 7.91 [t, 1H]; 7.93−8.02 [m, 2H]; 8.36 [d, 1H]; 9.73 [s, 1H, ^3J(PtH) = 24 Hz, N=CH]; 9.76 [s, 1H, ^3J(PtH) = 29 Hz, N=CH]. ^{19}F NMR: δ = −78.8 (s); −79.0 (s).

***R,R/S,S-trans*-1,2-[C_6H_{10}{N=CH-2-C_9H_6N(PtMe$_3$)}$_2$(μ-OSO$_2$CF$_3$)][SO$_3$CF$_3$], 13.** Yield = 81%. Anal. Calcd for $C_{28}H_{42}N_4O_6F_6S_2Pt_2$: C, 34.9; H, 3.6; N, 4.8. Found: C, 34.5; H, 4.0; N, 4.4. ^{1}H NMR (CD_2Cl_2): δ 0.89 [s, 3H, ^2J(PtH) = 83 Hz, Pt−Me]; 1.05 [s, 3H, ^2J(PtH) = 83 Hz, Pt−Me]; 1.50 [s, 3H, ^2J(PtH) = 67 Hz, Pt−Me]; 1.52 [s, 3H, ^2J(PtH) = 68 Hz, Pt−Me]; 1.60 [s, 3H, ^2J(PtH) = 68 Hz, Pt−Me]; ca. 1.42−1.80 [br m, 2H, Cy]; 1.75 [s, 3H, ^2J(PtH) = 69 Hz, Pt−Me]; 2.04 [br m, 3H, Cy]; 2.23 [br m, 1H, Cy]; 2.41 [br m, 1H, Cy]; 2.50 [br m, 1H, Cy]; 5.28 [m, 2H, NCH]; 7.69 [m, 2H]; 7.82 [m, 2H]; 7.93 [m, 2H]; 8.18 [d, 1H]; 8.44 [d, 2H]; 8.50 [d, 1H]; 8.58 [s, 2H]; 10.05 [s, 1H, ^3J(PtH) = 25 Hz, N=CH]; 10.10 [s, 1H, ^3J(PtH) = 30 Hz, N=CH]. ^{19}F NMR: δ −78.9 (s); −79.2 (s).

***cis*-1,2-[C_6H_{10}{N=CH-2-C_5H_4N(PtMe$_3$)}$_2$(μ-BH$_4$)][SO$_3$CF$_3$], 15.** To a solution of complex **10** (0.0375 g, 0.032 mmol) in THF (30 mL) was added 4−5 equiv of $NaBH_4$. The very pale yellow solution slowly turned to a more intense yellow color. After ca. 15 h, a blackened yellow solution was obtained and the solvent was evaporated under reduced pressure to give a dark brown residue. The residue was triturated with several portions of pentane (3 × 20 mL) and then dried under vacuum to give a brown powder. Extraction of the brown solid with CH_2Cl_2 and filtration of the extracts over Celite to remove platinum metal gave a bright yellow solution. Removal of the solvent under reduced pressure yielded the yellow product. Yield = 0.024 g (80%). Anal. Calcd for $C_{25}H_{42}N_4BO_3F_3SPt_2$: C, 32.1; H, 4.5; N, 6.0. Found: C, 32.3; H, 4.4; N, 5.5. ^{1}H NMR (CD_2Cl_2): δ −3.0 [br s, 4H, μ-BH_4]; 0.57 [s, 6H, ^2J(PtH) = 73 Hz, Pt−Me]; 1.13 [s, 6H, ^2J(PtH) = 68 Hz, Pt−Me]; 1.19 [s, 6H, ^2J(PtH) = 69 Hz, Pt−Me]; 1.72 [br m, 2H, Cy]; 1.84 [br m, 2H, Cy]; 2.14 [br m, 2H, Cy]; 2.54 [br m, 2H, Cy]; 4.85 [br s, 2H, NCH]; 7.58 [m, 2H]; 8.06 [t d, 2H]; 8.53 [d, 2H]; 8.61 [d, 2H]; 9.52 [s, 2H, ^3J(PtH) = 32 Hz, N=CH]. ^{19}F NMR (CD_2Cl_2): δ −79.2 (s). ^{11}B NMR (CD_2Cl_2): δ −22.4 (br s). IR (Nujol, NaCl, cm^{-1}): ν 2467 (w); 2406 (w); 1991 (vs br); 1606 (m); 1282 (s); 1265 (s); 1166 (s); 1036 (s); 781 (m); 642 (s).

***cis*-1,2-[C_6H_{10}{N=CH-2-C_5H_4N(PtMe$_3$)}$_2$(μ-Cl)][SO$_3$CF$_3$], 16.** Complex **16** cocrystallized with **15** as single crystals from a CH_2Cl_2 solution of complex **15** layered with pentane. ^{1}H NMR (CD_2Cl_2): δ 0.57 [s, 6H, ^2J(PtH) = 78 Hz, Pt−Me]; 1.10 [s, 6H, ^2J(PtH) = 67 Hz, Pt−Me]; 1.27 [s, 6H, ^2J(PtH) = 69 Hz, Pt−Me]; 4.91 [br s, 2H, NCH]; 7.58 [m, 2H]; 8.03 [t d, 2H]; 8.53 [d, 2H]; 9.47 [s, 2H, ^3J(PtH) = 30 Hz, N=CH].

***R,R/S,S-trans*-1,2[C_6H_{10}{N=CH-2-C_5H_4N(PtMe$_3$(PPh$_3$))}$_2$]-[SO$_3$CF$_3$]$_2$, 17.** To a yellow solution of **11** (0.044 g, 0.041 mmol) in THF (10 mL) was added PPh_3 (0.022 g, 0.083 mmol). The solution was stirred for 15 h, concentrated to ca. 2−3 mL under reduced pressure, followed by the addition of pentane (30 mL) to precipitate a very pale yellow powder. The product was washed extensively with pentane (3 × 10 mL) and dried under vacuum. Yield = 0.059 g (89%). Anal. Calcd for $C_{62}H_{68}N_4P_2O_6F_6S_2Pt_2$: C, 46.7; H, 4.3; N, 3.5. Found: C, 47.2; H, 4.6; N, 3.7. ^{1}H NMR (CD_2Cl_2): δ 0.12 [d, 6H, ^2J(PtH) = 59 Hz, ^3J(PH) = 7 Hz, Pt−Me]; 0.98 [d, 6H, ^2J(PtH) = 69 Hz, ^3J(PH) = 8 Hz, Pt−Me]; 1.62 [d, 6H, ^2J(PtH) = 67 Hz, ^3J(PH) = 8 Hz, Pt−Me]; 4.79 [m, 2H, NCH]; 7.18−7.50 [br m, 32H]; 8.02 [m, 4H]; 8.37 [d, 2H]; 9.55 [s, 2H, ^3J(PtH) = 33 Hz, N=CH]. ^{31}P NMR (CD_2Cl_2): −4.2 [s, ^1J(PtP) = 992 Hz]. ^{19}F NMR (acetone-d_6): −77.9 (s).

X-ray Structure Determinations. Data were collected by using a Nonius Kappa-CCD diffractometer with COLLECT (Nonius, 1998) software. Crystal data and refinement parameters are listed in Table 10. Data were scaled using SCALEPACK (Nonius, 1997), and empirical absorption corrections were applied using redundant data and XPREP (SHELXTL 5.03). Full-matrix least-squares refinement on F^2 was performed after solving using Patterson methods and the solution package SHELXTL 5.03 (Sheldrick, G. M., Madison, WI). Positional and thermal parameters, all bond distances and angles, anisotropic thermal parameters, and hydrogen atom coordinates have been included in the Supporting Information.

Crystals of **7a** were grown from a mixture of **7a** and **7b** at low temperature from a CD_2Cl_2 solution, and a crystal was mounted on a glass fiber. Crystals of **8b** were grown from a saturated solution of CD_2Cl_2 and were mounted as above. Unit cell parameters were calculated from reflections obtained from 10 consecutive data images collected at φ intervals of one degree using DENZO (Nonius, 1998). One full hemisphere of data were collected by incremental φ scans of one degree followed by one degree ω scans to capture cusp data. Analysis of systematic absences indicated either of the monoclinic space groups *Cc* and *C*2/*c*, and the centric option was chosen and refined successfully.

Crystals of **8f** were grown by slow diffusion of pentane into a methylene chloride solution. An orange plate was mounted on a glass fiber. The reflection data suggested a triclinic cell, and the structure was solved successfully in $P\bar{1}$. There were two independent molecules in the asymmetric unit. The anions were disordered at the CF_3 groups, and so the CF_3 groups were modeled as two-half-occupancy moieties which were roughly staggered with respect to each other. The fluorine atoms were kept isotropic, and the atomic distances were fixed (C−F = 1.33 Å; F−F = 2.17 Å). All other non-hydrogen atoms were refined with anisotropic thermal parameters. The hydrogen atoms were calculated geometrically and were either riding, or in the case of methyl groups, riding as rigid groups on their respective carbon atoms. The water of solvation was modeled as a single anisotropic oxygen atom.

Table 10. Crystallographic Details

	7a	8b	8f	9b
formula	$C_{24}H_{38}I_2N_4Pt_2$	$C_{24}H_{38}I_2N_4Pt_2$	$C_{26}H_{38}F_3IN_4O_{2.5}Pt_2$	$C_{33.50}H_{45}Cl_3I_2N_4Pt_2$
fw	1026.56	1026.56	1020.68	1254.07
temp, K	125(2)	295(2)	294(2)	293(2)
wavelength, Å	0.71073	0.71073	0.71073	0.71073 Å
cryst syst	triclinic	monoclinic	triclinic	triclinic
space group	$P\bar{1}$	$C2/c$	$P\bar{1}$	$P\bar{1}$
unit cell dimens				
a, Å	10.262(2)	25.0880(4)	14.2370(3)	12.5751(3)
b, Å	11.777(2)	8.8818(2)	14.7143(3)	12.6532(3)
c, Å	12.965(3)	14.5842(4)	16.0584(3)	13.5138(2)
α, deg	100.98(3)		72.1290(10)	86.4738(12)
β, deg	101.78(3)	112.4460(10)	83.9630(10)	83.1055(12)
γ, deg	105.64(3)		85.0240(10)	74.6706(10)
volume, Å^3	1426.2(5)	3003.55	3178.69(11)	2057.76(8)
Z	2	4	4	2
d(calc), Mg/m^3	2.391	2.27	2.133	2.024
abs coeff, mm^{-1}	11.982	11.378	9.811	8.513
F(000)	944	1888	1912	1174
no. of reflns collcd	10 636	26 371	33 601	11 939
no. of ind reflns	5026 [R(int) = 0.0710]	2647 [R(int) = 0.0542]	12 870 [R(int) = 0.0810]	8298 [R(int) = 0.0450]
no. of data/ restraints/ params	5026/0/295	2639/0/146	12870/24/700	8298/0/421
GOOF on F^2	1.025	1.029	0.983	1.064
final R [$I > 2(I)$]	R1 = 0.453, wR2 = 0.1054	R1 = 0.0406, wR2 = 0.1092	R1 = 0.0632, wR2 = 0.1766	R1 = 0.0378, wR2 = 0.1141
R (all data)	R1 = 0.0720, wR2 = 0.1153	R1 = 0.0546, wR2 = 0.1289	R1 = 0.0733, wR2 = 0.1852	R1 = 0.0421, wR2 = 0.1177
largest diff peak, hole, e Å^{-3}	2.054 and −1.910	1.637 and −1.601	2.216 and −2.497	2.333 and −2.093

	10	11	14	15/16
formula	$C_{26.5}H_{38.5}Cl_{1.5}F_6N_4O_6Pt_2S_2$	$C_{26}H_{38}F_6N_4O_6Pt_2S_2$	$C_{26}H_{38}F_6N_4O_9Pt_2S_2$	$C_{25}H_{40}B_{0.5}Cl_{0.5}F_3N_4O_3Pt_2S$
fw	1130.59	1070.90	1118.90	946.98
temp, K	292(2)	294(2)	292(2) K	292(2)
wavelength, Å	0.71073	0.71073	0.71073	0.71073
cryst syst	triclinic	triclinic	monoclinic	orthorhombic
space group	$P\bar{1}$	$P\bar{1}$	$P2(1)/c$	$Pca2(1)$
a, Å	10.8287(2)	13.6927(10)	19.3347(10)	31.7784(3)
b, Å	17.2696(4)	15.9762(12)	17.7954(7)	10.9013(2)
c, Å	21.5413(5)	17.9748(13)	11.5549(6)	18.0375(3)
α, deg	76.3840(10)	77.642(4)		
β, deg	82.3350(10)	69.131(4)	94.771(2)	
γ, deg	73.8140(10)	89.997(4)		
volume, Å^3	3750.06(14)	3576.5(5)	3961.9(3)	6248.66(17)
Z	4	4	4	8
d(calc), Mg/m^3	2.003	1.989	1.876	2.013
abs coeff, mm^{-1}	7.743	8.004	7.236	9.105
F(000)	2164	2048	2144	3616
no. of reflns collcd	31 123	29 196	24 813	50 907
no. of ind reflns	14 032 [R(int) = 0.0520]	13 733 [R(int) = 0.0900]	3989 [R(int) = 0.0950]	6575 [R(int) = 0.0750]
no. of data/ restraints/ params	14032/0/865	13733/0/841	3989/12/436	6575/11/723
GOOF on F^2	1.019	1.019	1.041	1.052
final R [$I > 2(I)$]	R1 = 0.0412, wR2 = 0.1001	R1 = 0.0816, wR2 = 0.1433	R1 = 0.0532, wR2 = 0.1377	R1 = 0.0363, wR2 = 0.0886
R (all data)	R1 = 0.0540, wR2 = 0.1081	R1 = 0.1835, wR2 = 0.1780	R1 = 0.0647, wR2 = 0.1484	R1 = 0.0413, wR2 = 0.0920
largest diff peak, hole, e Å^{-3}	1.576 and −1.725	1.748 and −0.977	1.256 and −1.033	1.796 and −1.532

Crystals of **9b** were grown from slow diffusion of pentane into a CD_2Cl_2 solution. An orange shoebox shaped crystal was mounted in a capillary; 1.5 methylene chlorides of solvation were found in the asymmetric unit.

Crystals of **10** were grown from slow diffusion of pentane into a $CDCl_3$ solution. A colorless crystal was mounted in a capillary. One chloroform of solvation was found in the asymmetric unit, which contained two distinct platinum dimers with their respective anions. Crystals of **11** were grown from slow diffusion of pentane into a methylene chloride solution. A clear twinned needle was cut, and a fragment was mounted in a capillary. The refinement showed two molecules per asymmetric unit.

Crystals of **14** were grown from slow diffusion of diethyl ether into a CD_2Cl_2 solution. A colorless block suitable for X-ray analysis was selected and mounted in a capillary. The refinement was straightforward except for the cyclohexyl group. This was modeled by two cyclohexyl groups at half-occupancy. All other non-hydrogen atoms were refined with anisotropic thermal parameters. The hydrogen atoms were calculated geometrically and were riding on their respective carbon atoms. Three molecules of water were found in the asymmetric unit: one on each of the platinum atoms and one off on its own. These were all modeled solely by an anisotropic oxygen, as the hydrogen atoms of the water molecules were not found. The largest residual electron den-

sity peak (1.256 e/Å^3) was associated with one of the platinum atoms.

Crystals of **15**/**16** were grown from slow diffusion of pentane into a CD_2Cl_2 solution of **15**, with partial reaction with solvent during crystallization. A yellow crystal was mounted in a capillary. The unit cell parameters were calculated and refined from the full data set. The reflection data were consistent with an orthorhombic system: *Pca*2(1). All non-hydrogen atoms were refined with anisotropic thermal parameters, with the exception of the boron atom. The hydrogen atoms were calculated geometrically and were riding on their respective carbon atoms. Two molecules were found in the asymmetric unit: one with a chlorine atom bridging the platinum atoms and the other with a BH_4 unit bridging the two platinum atoms. The boron atom and one of the hydrogens were found in the difference map. The BH_4 unit was fixed as a tetrahedron by setting the B−H distances to 1.30 Å and the H−H distances to 2.12 Å. The structure was solved as a racemic twin, and the BASF parameter was refined to a value of 0.526.

Acknowledgment. We thank NSERC (of Canada) for financial support and for a Postgraduate Scholarship to C.R.B.

Supporting Information Available: Tables of X-ray data for complexes **7a**, **8b**, **8f**, **9b**, **10**, **11**, **14**, and **15**/**16**. This material is available free of charge via the Internet at http://pubs.acs.org.

OM000108N